Safer Offshore Energy Systems 3 Final Report

Project Title: Passive acoustic technique for detecting, locating, and characterizing hydrocarbon leakages
Award Amount: $591,060
Awardee: University of Mississippi
Award Start Date: 12/01/17
Award End Date: 11/30/20
NAS Grant ID: 200008860

Project Director: Zhiqu Lu
Affiliation: University of Mississippi

Project Key Personnel:

- Likun Zhang, National Center for Physical Acoustics, University of Mississippi
- Lei Cao, Department of Electrical Engineering, University of Mississippi

I. PROJECT SUMMARY (from proposal)

In this project, the National Center for Physical Acoustics and the Department of Electrical Engineering at the University of Mississippi propose to develop a hydrophone network-based real-time passive monitoring system for detecting, locating, and characterizing hydrocarbon leakages undersea. This project directly addresses the purpose of reducing the systemic risks leading to uncontrolled hydrocarbon release set by the Gulf Research Program.

The U.S. outer continental shelf is a major source of energy for the United States. Oil and gas production in the Gulf of Mexico increases the risk of underwater oil spills at greater water depths and drilling wells. These hydrocarbons leakages can be caused by either natural events, such as seeping from fissures in the ocean seabed, or by anthropogenic accidents, such as leaking from broken wellheads and pipelines. In order to improve safety and reduce the environmental risks of offshore oil and gas operations, the Bureau of Safety and Environmental Enforcement recommended the use of real-time monitoring. An early warning system for detecting, locating, and characterizing hydrocarbon leakages is essential for preventing the next oil spill as well as for seafloor hydrocarbon seepage detection. Existing techniques, such as an acoustic array apparatus, hydrostatic pressure tests, and acoustic sonars, either cannot determine the exact location or need to be deployed in a close range of the leakage location.

With the objective of leakage detection and localization, our approach consists of recording and modeling the acoustic signals induced by the oil-spill and implementing advanced signal processing and triangulation localization techniques with a hydrophone network. In an oil spill event, the leaked hydrocarbon is injected into seawater with huge amounts of discharge at high speeds. With mixed natural gases and oils, this hydrocarbon leakage creates underwater sound through two major mechanisms: shearing and turbulence by a streaming jet of oil droplets and gas bubbles; and bubble oscillation and collapse. These acoustic emissions can be recorded by hydrophones in the water column at far distances. They will be characterized and differentiated from other underwater noises through

their unique frequency spectrum, evolution and transportation processes and recording positions, and further be utilized to detect and position the leakage locations.

Tasks of this project are:
1. Conduct a laboratory study to simulate hydrocarbon leakages and their induced sound under controlled conditions, and to establish the correlation between frequency spectra and leakage properties, such as oil-jet intensities and speeds, bubble radii and distributions, and crack sizes.
2. Implement and develop acoustic bubble modeling for estimating features and strength of the oil leakage.
3. Develop a set of advanced signal processing and triangulation algorithms for leakage detection and localization.

Given the size of the oil business in the Gulf area, this project could have a tremendous impact. The scientific findings will be promptly disseminated through various ways. The research team will closely collaborate with GOWell LLC throughout the experimentation. Further testing in the ocean, along with prototyping and commercializing efforts, will be immediately pursued upon the success of the project.

II.   PROJECT SUMMARY (from final report)

Oil and gas production in the Gulf of Mexico increases the risk of underwater oil spills at greater water depths and drilling wells. These hydrocarbons leakages can be caused by either natural events, such as seepage from fissures in the ocean seabed, or by anthropogenic accidents, such as broken wellheads and pipelines. In order to improve safety and reduce the risks posed by offshore oil and gas operations, an early warning system for detecting, locating, and characterizing hydrocarbon leakages is essential.

In this project, the National Center for Physical Acoustics, collaborating with the Department of Physics and the Department of Electrical Engineering at the University of Mississippi, has developed a hydrophone network-based real-time passive monitoring system for detecting, locating, and characterizing hydrocarbon leakages. In an oil spill event, the leaked hydrocarbon, comprised of mainly methane gas, is injected into seawater with huge amounts of discharge at high speeds. This leakage creates underwater sounds due to bubble oscillations. These acoustic emissions can be recorded by hydrophones in the water column at far distances. Our approach consists of recording and modeling the acoustic signals in a laboratory facility and implementing advanced signal processing and localization techniques. This project directly addresses the purpose of reducing the systemic risks leading to uncontrolled hydrocarbon release set by the Gulf Research Program.

The three tasks of this project are:
1. Conduct a laboratory study to simulate hydrocarbon leakages and their induced sound under controlled conditions, and to establish the correlation between frequency spectra and leakage properties, such as oil-jet intensities and velocities, bubble radii and distributions, and crack sizes.
2. Implement and develop acoustic bubble modeling for estimating features and strength of the oil leakage.

3. Develop a set of advanced signal processing and triangulation algorithms for leakage detection and localization.

With the completion of the project, the developed oil-induced sound mechanism/dynamics, detection metrics, oil-leakage characterization, and localization technology could be applied to design a prototype low-cost hydrophone network-based real-time monitoring system that covers a large area. Given the proliferation of oil industry operations in the Gulf area, these research results could have tremendous impacts on science, technology, oil industries, and the environment.

III. PROJECT RESULTS

Accomplishments

For the task of laboratory study, the experimental setup consisted of a water tank (Figure 1-1), two bubble generation apparatuses (Figure 1-2), two active hydrophones, a passive hydrophone network, five passive hydrophone arrays (Figure 1-3), an instrument control and data acquisition system (Figure 1-4), and an underwater camera (Figure 1-1). Two types of oil leakages were simulated through two bubble generation methods. The first was "constant flow bubbles", which simulates oil well and pipe-line breaches. In this case, the bubbles were generated continuously at constant flow rates by using a compressed gas cylinder (Figure 1-5a). The second bubble generation scheme was "a few bubbles", which simulates oil seepage from the seafloor. For this case, the bubbles were generated by a syringe pump operating at very low flow rates to create a single or just a few bubbles (Figure 1-6a). Two gases were tested: nitrogen and methane. The latter is the major component of natural gases. The bubble sounds, recorded by passive hydrophones (Figure 1-5b, Figure 1-6b), were transformed into frequency spectra (Figure 1-5c, Figure 1-6c) through fast Fourier transform for signal analysis. Digital camera movies were recorded, which captured the processes of bubble leakages. In order to establish the correlation between frequency spectra and oil leakage properties, the tests were conducted under different pressures, flow rates, jet velocities, and diameters of needles that were used to simulate the crack sizes. The signal analysis was performed by calculating the total energy for the cases of constant flow bubbles (Figure 2-1) and the resonant frequency for the cases of a few bubbles (Figure 2-2). It was found that (1) the resonant frequency decreased nonlinearly with the needle diameter (Figure 2-3) and (2) the sound intensity in terms of the total energy increased with the increase of the flow rate and the jet velocity (Figure 2-1a and Figure 2-1b). These observations are of significance for assessing the degree of oil leakages. Qualitatively speaking, if hydrophones in the water column record large intensity sounds, then an oil leakage with high flow rate and high jet velocity is indicated. If the recorded sound has low frequency components, large crack sizes are indicated.

In addition to the bubble oscillation mechanism, a second oil-spill related underwater sound mechanism was studied. A peristatic pump was employed to create a water streaming jet with pre-defined flow rates using tap water. Syringe needles with different diameters were tested. It was found that no significant sound was detected within the flow rate range for all needles tested. It is therefore concluded that the underwater sound created by a steaming jet of pure liquids is negligible compared to the sound created by bubble oscillations.

For the task of acoustic bubble modeling, we implemented the theory of bubble dynamics to understand the data taken from the above experiments. We considered (1) the dependence of the resonant frequency on the size of the crack, (2) the dependence of the sound intensity in terms of the total energy on the oil leak flow rate and jet velocity, and (3) the bubble size distribution. In the cases of a few bubbles, it was found that the resonant frequency is inversely proportional to the one third power of the needle diameter (Figure 2-3a), which is in good agreement with theoretical bubble dynamics (Longuet-Higgins, et al, 1991). It was also found that the resonant frequency is linearly proportional to the inverse effective bubble radius (Figure 2-3b). In the cases of constant flow bubbles, an empirical relationship was established among the total energy, flow rate, and needle diameter, i.e., the total energy is proportional to the square of the flow rate and inversely proportional to the cube of the needle diameter (Figure 2-1c). This empirical relationship can be further converted into a simple equation indicating that the total energy is proportional to the product of the jet-velocity and total number of bubbles (Figure 2-1d). This new equation provides better physical description of the bubble sound mechanism than the empirical relationship, as it indicates that the bubble sound energy is dominated by the jet velocity. Also in the cases of constant flow bubbles, the injected gases formed a cloud of bubbles with different bubble sizes. The induced bubble sound featured a broadband frequency spectrum with several distinctive frequency peaks that are related to bubble sizes (Figure 2-4). Using a Minnaert resonant frequency formula (Minnaert, 1933) and the sound pressure generated by a single bubble model (Leighton and Walton, 1987), the bubble size distributions were estimated (Figure 2-5 and Figure 2-6). The above acoustic bubble modeling enhanced our understanding of the underlying mechanisms of bubble-induced sounds and will be applied to guide the assessment of the features of oil leakage from the recorded sound signals.

For the task of localization, a randomly distributed passive hydrophone network with seven passive hydrophones, two active hydrophone sources, and two bubble sources were positioned at different locations of the water tank (Figure 1-3). The time difference of arrivals (TDOAs) determined from the first arrival were used as input parameters for localization algorithms (Figure 3-1). Two types of algorithms were developed and tested: Linear Least Square Estimation (LLSE, Figure 3-2) and Nonlinear Least Square Estimation (NLS, Figure 3-3). The estimated locations were in good agreement with the true source locations (Figure 3-4). In the field, for an existing oil leakage source, the underwater sound will be continuously generated. In this situation, it is difficult to determine the first arrivals of the oil leakage sounds at different sensing hydrophones, and it is more desirable to study the localization methods based on direction of arrival (DOA). For this purpose, five liner hydrophone arrays were employed. Several localization algorithms using the DOAs were developed and tested, including generalized cross-correlation with phase transform (GCC-PHAT) and subspace based MUSIC algorithms. However, several technical difficulties emerged, including (1) multipath and reverberation and (2) near field effect. Despite the many efforts that were made to suppress these effects, reliable DOAs were not obtained. Realizing the limitations of the small water tank, we moved our test site to a swimming pool in the Recreation Center of the University of Mississippi in an attempt to achieve far-field conditions (Figure 3-5). A few preliminary tests were conducted. However, these indoor measurements still suffered from adverse factors, including noise interference from a pool filtration pump, air-conditioners, and nearby machinery, as well as significant multipath and reverberation effects. Due to the outbreak of COVID-19, the swimming pool test was suspended. In this unanticipated situation, another localization technique not planned in the initial proposal was developed. Instead of using the DOAs-based methods

that require acoustic propagation in a free field or in an anechoic environment, a Green's function method was adopted to deal with the multipath/reverberation environment and the near field conditions of the water tank. This technique is based on an analytical modeling of the acoustic field of the water tank, i.e., the Green's function of the water tank (Novak, et al., 2018). The localization algorithm compares two spectra ratios: the spectra ratio between the signals measured by hydrophones at two locations and the spectra ratio between the theoretical Green's functions at the same locations (Novak, et al., 2019). The Green's functions at all possible source locations (thousands) in the form of grids in the water tank were calculated using known tank physical properties including the geometric size of the tank, the sound speed and the thickness of the tank wall (Figure 3-6). The locations of the bubble source were determined by the highest probability of matching (Figure 3-8). Three different water tank models were tested and compared, including the Dirichlet model, a model including leakage through the wall, and a newly proposed model developed in this study. Several bubble sources at different locations were tested for localization. The estimated results were in satisfactory agreement with the true source locations (Figure 3-9). Among the three models, the newly proposed model demonstrated the best localization performance. However, it should be noted that the Green function method can only be used specifically for the water tank. For a more realistic situation involving an oil spill, conventional localization algorithms, such as the TDOA-based; the DOA-based and the energy-based method; or other advanced algorithms such as neutral network, matched field processing (MFP) methods should be developed. And for that case, a much larger test site, like a lake or ocean, would be needed. One possible site might be Sardis Lake, a large 98,520 acre reservoir 12 miles away from the university campus. That could be the future research work for the next proposal.

In summary, a laboratory study to simulate hydrocarbon leakages was conducted under controlled conditions such as pressures, flow rates, jet velocities, and crack sizes. Two types of oil leakages were tested to simulate oil seepages either from seafloors or from oil well and pipe-line breaches. Two types of gases were investigated: nitrogen and methane. The latter is the major component of natural gases. The bubble sounds were recorded by the passive hydrophones and transformed into frequency spectra through the fast Fourier transform for signal analysis. It was found that (1) the resonant frequency decreased nonlinearly with the diameter of needle and (2) the sound intensity in terms of the total energy increased with both the flow rate and the jet velocity. These observations are of significance for assessing the properties of oil leakages in terms of crack size, flow rate, and jet velocity. It was also found that oil leakage –induced underwater sound was dominated by bubble oscillations rather than by jet streaming.

For the task of acoustic bubble modeling, we implemented the theory of bubble dynamics to analyze the data taken from the above experiments. We considered (1) the dependence of the resonant frequency on the size of crack, (2) the dependence of the sound intensity in terms of the total energy on the flow rate and jet velocity, and (3) the bubble size distribution. Several correlations between the oil leakage properties and acoustic responses were established and interpreted. The outcome of the modeling enhanced our understanding of the underlying mechanisms of bubble-induced sounds and will be applied to guide the assessment of the features of oil leakage from the recorded sound signals.

For the task of localization, the time difference of arrivals determined from the first arrival were used as input parameters for localization algorithms. Two types of algorithms were developed and tested: LLSE

and NLS Estimation. It was also found that the proposed DOA-based localization methods were not suitable for this small-scale water tank due to strong multipath, reverberation, and near field effects. To overcome these technical challenges, an approach that was based on analytical modeling the acoustic field of the water tank, i.e., the Green's function of the water tank, was developed and tested. The estimated locations using both the TDOA and Green's function techniques were in good agreement with the true source locations. For a more realistic situation involving an oil spill, conventional localization algorithms, such as the TDOA-based, the DOA-based and the energy-based method, or other advanced algorithms, such as neutral network, MFP methods, should be developed. And for that case, a much larger test site, like a lake or ocean, would be needed.

Implications

Oil and gas production in the Gulf of Mexico increases the risk of oil spills at greater water depths and drilling wells. An early warning system for detecting, locating, and characterizing hydrocarbon leakages is essential for oil spill detection as well as for seafloor hydrocarbon seepage detection. In this project, a passive hydrophone network-based system for detecting, locating, and characterizing hydrocarbon leakages has been developed in the laboratory. With the scientific knowledge gained from this project, including detection metrics, oil-leakage characterization, and localization technology, a prototype, network-based hydrophone monitoring system could be developed for use in the ocean. The ultimate goal of the study is to improve safety of offshore oil and gas operations and systems, which directly addresses the purpose of reducing the systemic risks leading to uncontrolled hydrocarbon release set by the Gulf Research Program.

This research has yielded much scientific insight into the sound mechanisms of leakages, their relationship to the causative properties, the complexity of leakage sound propagation, and the localization methods for the leakage position.

During the project, it was found that the oil leakage-induced underwater sounds recorded by the passive hydrophone network can be used to determine the locations of oil leakages and be further analyzed to estimate the leakage properties such as flow rates, jet velocities, crack sizes, and bubble size distributions.

Researchers, educators, and the for-profit private sector would be most likely interested in the finding of the project. The developed acoustic bubble modeling enhanced the understanding of the mechanisms of bubble-induced sounds, which would be valuable for researchers and educators who are working or educating in the relevant areas. The correlation between acoustic responses and oil-leakage properties can be applied to predict the degree of oil-leakage by oil industries. The basic research on bubble sound mechanisms may be extended under more realistic ocean conditions, such as high pressures, low temperatures, and salinities. The localization concept and methodology used in this project can be further improved and applied to a field test site and attract the attention of other researchers, oil industries, and for-profit private company for investing, developing, and improving the practical prototype of the passive acoustic monitoring system.

With the scientific knowledge gained from this project, including detection metrics, oil-leakage characterization, and localization technology, a prototype network-based hydrophone monitoring

system could be developed for field use. With follow-on funding, investigators of this project team, in collaboration with industry stakeholders, could pursue development and deployment of an in-situ detection and localization system at Sardis Lake, which is just 12 miles away from the University of Mississippi.

Given the proliferation of oil industry operations in the Gulf area, these research results could have tremendous impacts on science, technology, oil industries, and the environment.

Education and Training
Number of students, postdoctoral scholars, or educational components involved in the project:
- Undergraduate students: 0
- Graduate students: 4
- Postdoctoral scholars: 0
- Other educational components: 0

IV.   DATA AND INFORMATION PRODUCTS
This project produced data and information products of the following types:
- Data
- Information Products
- Scholarly publications, reports or monographs, workshop summaries or conference proceedings
- Websites or data portals
- Models or simulations

DATA

Data Management Report:
See Data Management Report below.

Relationships Between Data Sets:
There are three types of data sets: 1. test data set, 2. Modeling data set, and 3. localization data set. They are listed as follows.

1. Test Data Report:
   - For nitrogen-constant flow tests, the data are raw recorded underwater sounds generated by constant flow bubbles.
     File name: Tank-18-10-08-10-52-38-G14-cons-2.5psi-100 kHz - Gain100.xls
     Note: Tank-year-month-day-hour-min-sec-needle gauge number-constant flow test-pressure-sampling frequency-gain

   - For nitrogen-a few bubble tests, the data are raw recorded underwater sounds generated by a few bubbles.
     File name: Tank-18-07-30-08-12-50-G18-single-30uL-250 kHz.xls
     Note: Tank-year-month-day-hour-min-sec-needle gauge number-a few bubbles-flow rate-

sampling frequency

- For nitrogen-constant flow video, the videos were recorded during constant flow bubble tests.
  File name: G16-5 PSI.mov
  Note: Needle gauge number-pressure

- For nitrogen-a few bubble video, the videos were recorded during a few bubble tests.
  File name: G16-single bubble-1.mov
  Note: Needle gauge number-a few bubbles

- For nitrogen-constant flow rates, the data was flow rates measured during constant flow tests.
  File name: 468493-1_10-03-2018_13-30-47_G12_2.5psi.txt
  Note: Test ID-month-date-year-hour-min-sec-needle gauge #-pressure

- For nitrogen-resonant frequency histograms, the histograms were obtained by processing data from nitrogen-a few bubble tests.
  File name: Histogram-nitrogen.doc
  Note: The doc file contains all images of the resonant frequency histograms for a few bubble nitrogen tests.

- For nitrogen-resonant frequency, the data was generated by processing data from Histogram-nitrogen.doc
  File name: Resonant F-nitrogen.xls
  Note: the resonant frequency vs needle diameter

- For nitrogen-total energy vs flow rate and jet velocity, the data was generated by processing data from nitrogen-constant flow tests, flow rate measurement, and needle diameters.
  File name: Total energy -nitrogen.xls
  Note: the file contains data and figures for total energy vs flow rate and total energy vs jet velocity

- For methane-constant flow tests, the data are raw recorded underwater sounds generated by constant flow bubbles.
  File name: Tank-18-11-12-09-33-24-G18-CH4-5psi-100 kHz - Gain100 - 40dB.xls
  Note: Tank-year-month-day-hour-min-sec-needle gauge number-channel number-pressure-sampling frequency-gain

- For methane-a few bubble tests, the data are raw recorded underwater sounds generated by a few bubbles.
  File name: Tank-18-11-28-22-33-55-200ul-G16-single-250 kHz-Gain1000-60dB.xls
  Note: Tank-year-month-day-hour-min-sec-flow rate-needle gauge number-single bubble-sampling frequency-gain

- For methane-constant flow rates, the data are raw flow rates measured during constant flow tests.
  File name: 468493-1_11-12-2018_17-46-16_CH4_G16_7psi.txt
  Note: Test ID-month-date-year-hour-min-sec-needle gauge #-pressure

- For methane-resonant frequency histograms, the histograms were obtained by processing data from methane-a few bubble tests.
  File name: Histogram-methane.doc
  Note: The doc file contains all images of the resonant frequency histograms for a few bubble methane tests.

- For methane-resonant frequency, the data was generated by processing data from Histogram-methane.doc
  File name: Resonant F-methane.xls
  Note: the resonant frequency vs needle diameter

- For methane-total energy vs flow rate and jet velocity, the data are processed by the methane constant flow tests, flow rate measurement, and needle diameters.
  File name: total energy -methane.xlsx
  Note: the file contains data and figure for total energy vs flow rate and total energy vs jet velocity

2. Modeling Data Report:
   - For methane-a few bubbles modeling, the histograms were obtained by processing data from methane-a few bubble tests.
     File name: Histogram-methane.doc
     Note: The doc file contains all images of the resonant frequency histograms for a few bubble methane tests.

   - For nitrogen-a few bubbles modeling, the histograms were obtained by processing data from methane-a few bubble tests.
     File name: Histogram-nitrogen.doc
     Note: The doc file contains all images of the resonant frequency histograms for a few bubble nitrogen tests.

   - For methane-a few bubbles modeling, the data was generated by processing data from Histogram-methane.doc
     File name: Resonant F-methane.xls
     Note: the resonant frequency vs needle diameter

   - For nitrogen-a few bubbles modeling, the data was generated by processing data from Histogram-methane.doc
     File name: Resonant F-nitrogen.xls

Note: the resonant frequency vs needle diameter

- For a few bubbles modeling, the result was obtained by analyzing the data from Resonant F-nitrogen.xls and Resonant F-methane.xls
  File name: a few bubbles-Peak frequency.jpg
  Note: the file contains the results for both Nitrogen and Methane gases.

- For methane-constant flow modeling, the data are processed by the methane constant flow tests, flow rate measurement, and needle diameters.
  File name: total energy -methane.xlsx
  Note: the file contains data and figure for total energy vs flow rate and total energy vs jet velocity

- For Methane-constant flow modeling, the data are raw recorded underwater sounds generated by constant flow bubbles.
  File name: Methane_G16.xlsx
  Note: Gas-type_Gauge-number.xlsx
- For Nitrogen- constant flow modeling, the data are raw recorded underwater sounds generated by constant flow bubbles.
  File name: Nitrogen_G16.xlsx
  Note: Gas-type_Gauge-number.xlsx

- For Nitrogen and Methane constant flow tests, the results were obtained by analyzing the data for the case of constant flow.
  File name: Results for constant flow bubbles.docx
  Note: The file contains all the results for the constant flow bubbles for both gases.

- For Nitrogen and Methane constant flow modeling, the result is obtained from the equation in the report.
  File name: constant flow bubbles-E0.jpg
  Note: The file contains the profile of the weighting function used in characterization.

- For Nitrogen and Methane constant flow modeling, the results were obtained by analyzing the data for the case of constant flow.
  File name: constant flow bubbles-Energy.jpg
  Note: The file contains the results for both two gases.

- For Nitrogen and Methane constant flow modeling, the results were obtained by analyzing the data for the case of constant flow.
  File name: constant flow bubbles-G14.jpg
  Note: The file contains the results for the needle of G14 for Nitrogen gas.

- For Nitrogen and Methane constant flow modeling, the results were obtained by analyzing the data for the case of constant flow.

File name: constant flow bubbles-NitrogenG14.jpg
Note: The file contains the results for the needle of G14 for Nitrogen gas.

- For Nitrogen and Methane constant flow modeling, the results were obtained by analyzing the data for the case of constant flow.
  File name: constant flow bubbles-Total.jpg

- For Nitrogen and Methane constant flow modeling, the results were obtained by analyzing the data for the case of constant flow for Methane gas.
  File name: Methane_Number_Percentage.jpg
  Note: The file contains the results for number percentage distribution for Methane gas.

- For Nitrogen and Methane constant flow modeling, the results were obtained by analyzing the data for the case of constant flow for Nitrogen gas.
  File name: Nitrogen _Number_Percentage.jpg
  Note: The file contains the results for number percentage distribution for Nitrogen gas.

- For Nitrogen and Methane constant flow modeling, the results were obtained by analyzing the data for the case of constant flow for Nitrogen gas.
  File name: Nitrogen_G14_NEW_number_percentage.jpg
  Note: The file contains the results for number percentage distribution for Nitrogen gas for G14 needle.

- For Nitrogen and Methane constant flow modeling, the results were obtained by analyzing the data for the case of constant flow for Nitrogen gas.
  File name: ProcedureNew.jpg
  Note: The file contains the procedure to compute number percentage distribution.

3. Localization Data Report:
   - For underwater TDOA-based Localization, the data are raw recorded by scattered receivers (CH2-CH7); source is the electrical sound S1.
     File name: Tank-18-10-02-09-54-42-S1-500 kHz.xls (Excel version)
     Tank-18-10-02-09-54-42-S1-500 kHz.BP (LabVIEW version)
     Note: Tank-year-month-day-hour-min-second- source #-sampling rate

   - For underwater TDOA-based Localization, the data are raw recorded by scattered receivers (CH1-CH6); source is the electrical sound S2.
     File name: Tank-18-05-05-14-29-34-S2-500 kHz.xls (Excel version)
     Tank-18-05-05-14-29-34-S2-500 kHz.BP (LabVIEW version)
     Note: Tank-year-month-day-hour-min-second- source #-sampling rate

   - For underwater TDOA-based Localization, the data are raw recorded by scattered receivers (CH2-CH7); source is the bubble sound S3.
     File name: Tank-18-07-18-06-37-G18-5 PSI-S3-500 kHz.xls (Excel version)

Tank-18-07-18-06-37-G18-5 PSI-S3-500 kHz.BP (LabVIEW version)
Note: Tank-year-month-day-hour-min-second- needle gauge #-gas pressure-source #-sampling rate

- For underwater TDOA-based Localization, the estimated localization results were obtained by processing data from TDOA-based localization data for sources S1-S4.
  File name: S1toS4_Source positions estimation_TDOA.jpeg
  Note: The jpeg file contains all the sources S1 to S4 location estimation results by two different TDOA-based localization methods (LLSE method, NLS [with Gauss–Newton Method])

- For underwater SpectraRatio-based Localization, the data are raw recorded by scattered receivers (CH1-CH7); source is the bubble sound S4.
  File name: Tank-20-06-13-07-26-01-S4-Bubble pulse-200 kHz.xlsx
  Note: Tank-year-month-day-hour-min-second-source-source type-sampling frequency

- For underwater SpectraRatio-based Localization, the data are raw recorded by scattered receivers (CH1-CH7); source is the bubble sound S4.
  File name: Tank-20-07-09-07-47-41-S4-Bubble continuous-20 kHz.xlsx
  Note: Tank-year-month-day-hour-min-second-source-source type-sampling frequency

- For underwater SpectraRatio-based Localization, the data are raw recorded by scattered receivers (CH1-CH7); source is the bubble sound S5.
  File name: Tank-20-07-10-08-16-27-S5-Bubble continuous-20 kHz.xlsx
  Note: Tank-year-month-day-hour-min-second-source-source type-sampling frequency

- For underwater SpectraRatio-based Localization, the data are raw recorded by scattered receivers (CH1-CH7); source is the bubble sound S5.
  File name: Tank-20-07-10-08-22-35-S5-Bubble pulse-20 kHz.xlsx
  Note: Tank-year-month-day-hour-min-second-source-source type-sampling frequency

- For underwater SpectraRatio-based Localization, the data are raw recorded by scattered receivers (CH1-CH7); source is the bubble sound S6.
  File name: Tank-20-07-28-07-14-51-S6-bubble pulse-20 kHz.xlsx
  Note: Tank-year-month-day-hour-min-second-source-source type-sampling frequency

- For underwater SpectraRatio-based Localization, the data are raw recorded by scattered receivers (CH1-CH7); source is the bubble sound S6.
  File name: Tank-20-07-28-07-16-11-S6-bubble continous-20 kHz.xlsx
  Note: Tank-year-month-day-hour-min-second-source-source type-sampling frequency

- For underwater SpectraRatio-based Localization, the data are raw recorded by scattered receivers (CH1-CH7); source is the bubble sound S7.
  File name: Tank-20-07-29-08-06-36-S7-bubble continous-20 kHz.xlsx

Note: Tank-year-month-day-hour-min-second-source-source type-sampling frequency

- For underwater SpectraRatio-based Localization, the data are raw recorded by scattered receivers (CH1-CH7); source is the bubble sound S7.
  File name: Tank-20-07-29-08-08-47-S7-bubble pulse-20 kHz.xlsx
  Note: Tank-year-month-day-hour-min-second-source-source type-sampling frequency

- For underwater SpectraRatio-based Localization, the coordinates of scattered receivers (CH1-CH7) and sources (S4-S7).
  File name: Receiver and Bubble Source Coordinates.xlsx
  Note: The excel file includes the coordinates of the sources (S4-S7) and scattered hydrophones (CH1-CH7) and Arrays (Array1-Array5).

- For underwater SpectraRatio-based Localization, the estimated localization result is obtained by processing data from SpectraRatio-based Localization data for source S7.
  File name: S7 Source position estimation_SpectraRatio_Proposed_Grid10.jpeg
  Note: The jpeg file contains the sources S7 location estimation result by SpectraRation-based localization method with Proposed model under water tank grids 10x10x10.

- For underwater SpectraRatio-based Localization, the estimated localization result is obtained by processing data from SpectraRatio-based Localization data for source S7.
  File name: S7 Source position estimation_DF in 3D space.jpeg
  Note: The jpeg file contains the sources S7 location estimation result and DF values in 3D space by under water tank grids 10x10x10 by SpectraRation-based localization method with Proposed model.

- For underwater SpectraRatio-based Localization, the estimated localization result is obtained by processing data from SpectraRatio-based Localization data for source S7.
  File name: S7 Source position estimation_DF in 2D space with z-axis is 1.09m.jpeg
  Note: The jpeg file contains the sources S7 location estimation result and DF values in 2D space with z-axis is 1.09m under water tank grids 10x10x10 by SpectraRation-based localization method with Proposed model.

- For underwater SpectraRatio-based Localization, the estimated localization results are obtained by processing data from SpectraRatio-based Localization data for source S4 to S7.
  File name: S4toS7 Source positions estimation_SpectraRatio_All_Grid10.jpeg
  Note: The jpeg file contains the S4 to S7 bubble sources location estimation results by spectra ratio-based localization method with three different models (Proposed model,M1 (Dirichlet Model), M2 (Including Leakage Through the Walls Model)) under water tank grids (10x10x10).

- For underwater SpectraRatio-based Localization, the estimated localization results are obtained by processing data from SpectraRatio-based Localization data for source S6.
  File name: S6 Source position estimation_SpectraRatio_All_Grid10and20.jpeg

Note: The figure contains the S6 bubble source location estimation results by spectra ratio-based localization method with three different models (Proposed model,M1 (Dirichlet Model), M2 (Including Leakage Through the Walls Model)) under water tank grids (10x10x10). Also includes the S6 bubble source location estimation results by spectra ratio-based localization method with three different models. (Proposed model,M1 (Dirichlet Model), M2 (Including Leakage Through the Walls Model)) under water tank grids (20x20x20).

- For underwater SpectraRatio-based Localization, the estimated localization result is obtained by processing data from SpectraRatio-based Localization data.
  File name: Results for Spectra Ratio-based method localization.docx
  Note: The file contains all the results for the SpectraRatio-based localization results.

Additional Documentation Produced to Describe Data:
A "2020 Data file ReadMe.doc" file was created to describe data listed in the above reporting table, which has been uploaded to both "Supplemental Report Materials" and to the data repository website at UM eGROVE (https://egrove.olemiss.edu/grpds).

The data, metadata, and programs and algorithms have been uploaded to the UM BOX under the name of "Gulf Research Project". (http://olemiss.edu.account.boc.com/login), to the data repository website of the UM eGROVE (https://egrove.olemiss.edu/grpds), and to one of the GRP listed repositories: NOAA's National Centers for Environmental Information (NCEI), using the Send2NCEI tool: https://www.nodc.noaa.gov/s2n/. For each set of data and for each program/algorithm/code, a ReadMe file has been created and uploaded, respectively.

Other Activities to Make Data Discoverable:
We have built a website (http://aduolp.olemiss.edu/) that summarizes the project including research background, research tasks, latest results, publications, references, and news and events. This website serves as a gateway for both peer researchers and the general public who are interested in this topic to gain further in-depth knowledge. New developments and data will be updated in the website semi-annually during the two-year maintenance period.

To ensure data access for others (e.g., researchers, decision makers, and the public), the final research data and scientific findings, and developed codes and readme documents have been submitted to one of the GRP listed repositories: NOAA's National Centers for Environmental Information (NCEI), using the Send2NCEI tool: https://www.nodc.noaa.gov/s2n. The submission package has been assigned Reference ID: WUXY24 and is under review.

Sensitive, Confidential, or Proprietary Data:
N/A

INFORMATION PRODUCTS

Information Products Report:
See Information Products Report below.

Citations for Project Publications, Reports and Monographs, and Workshop and Conference Proceedings:

- Likun Zhang, Xudong Fan, Zhiqu Lu, "Characterization of sound induced by bubbles released from nozzles", Gulf of Mexico Oil Spill & Ecosystem Science Conference, Feb. 3-6, 2020, Tampa, FL
- Xing Yang, Lei Cao, Zhiqu Lu, "Characterization and localization of oil leakages using passive acoustic techniques", Gulf of Mexico Oil Spill & Ecosystem Science Conference, Feb. 3-6, 2020, Tampa, FL
- Likun Zhang, Xudong Fan, Zhiqu Lu, "Characterization of sound induced by bubbles released from nozzles", 178th ASA 2-7 Dec, 2019, San Diego, CA
- Zhiqu Lu, Raviteja Chinnambeti, and Lei Cao, "Localization of bubble sources in a water tank for oil spill detection", 22nd Annual Gulf of Mexico Deepwater Technical Symposium, Aug. 27-29, New Orleans, LA, 2018.

Websites and Data Portals:

- We have built a website (http://aduolp.olemiss.edu) that summarizes the project including research background, research tasks, latest results, publications, references, and news and events. This website serves as a gateway for both peer researchers and general public who are interested in this topic to gain further in-depth knowledge. New developments and data will be updated in the website semi-annually during the two-year maintenance period.

- The data, metadata, and programs and algorithms have been uploaded to the UM BOX under the name of "Gulf Research Project". (http://olemiss.edu.account.boc.com/login), to the data repository website of the UM eGROVE (https://egrove.olemiss.edu/grpds), and to one of the GRP listed repositories: NOAA's National Centers for Environmental Information (NCEI), using the Send2NCEI tool: https://www.nodc.noaa.gov/s2n/. The submission package has been assigned Reference ID: WUXY24 and is under review.

- GRIIDC Data Portal: https://grp.griidc.org/research-group/about/911

The project website/data portal include: the project homepage (https://aduolp.olemiss.edu, the UM BOX under the name of "Gulf Research Project". (http://olemiss.edu.account.boc.com/login), the data repository of the UM eGROVE (https://egrove.olemiss.edu), and the GRP listed repositories: NOAA's National Centers for Environmental Information (NCEI), using the Send2NCEI tool: https://www.nodc.noaa.gov/s2n. These website/data portal and their contents will be maintained and new data and developments will be updated in the website semi-annually for at least two-years beyond grant period.

Additional Documentation Produced to Describe Information Products:
The programs and algorithms have been uploaded to the UM BOX under the name of "Gulf Research Project". (http://olemiss.edu.account.boc.com/login), to the data repository website of the UM eGROVE (https://egrove.olemiss.edu/grpds), and to one of the GRP listed repositories: NOAA's National Centers for Environmental Information (NCEI), using the Send2NCEI tool: https://www.nodc.noaa.gov/s2n. The submission package has been assigned Reference ID: WUXY24 and is under reviewing. For each

program/algorithm/code, a ReadMe file has been created and uploaded, respectively. They are listed below.

- Readme-Signal processing-energy sum file.txt
- Readme-Signal processing-windowed spectrum.txt
- Readme-Theory_single_bubble.txt
- Readme-Code for Bubble Distribution.txt
- Readme-Energy_total.txt
- Readme-alg_Green Function.txt
- Readme-alg_plot_DF.txt
- Readme-alg_preconditioning.txt
- Readme-alg_signal_feature.txt
- Readme-SpectraRatio Localization.txt
- Readme-Localization_TDOA_based_LLSE.txt
- Readme-Localization_TDOA_based_NLS_Guass_Newton.txt
- Readme-Obtain crosszero from waveforms.txt

Other Activities to Make Information Products Accessible and Discoverable:
We have built a website (http://aduolp.olemiss.edu) that summarizes the project including research background, research tasks, latest results, publications, references, and news and events. This website serves as a gateway for both peer researchers and general public who are interested in this topic to gain further in-depth knowledge. New developments and data will be updated in the website semi-annually during the two-year maintenance period.

To ensure data access for others (e.g., researchers, decision makers, and the public), within two months of the project end date, the final research data and scientific findings, and developed codes and readme documents have been submitted to one of the GRP listed repositories: NOAA's National Centers for Environmental Information (NCEI), using the Send2NCEI tool: https://www.nodc.noaa.gov/s2n. The submission package has been assigned Reference ID: WUXY24 and is under review.

Confidential, Proprietary, Specially Licensed Information Products:
N/A

V.   PUBLIC INTEREST AND COMMUNICATIONS

<u>Most Exciting or Surprising Thing Learned During the Project</u>
Oil production in the Gulf of Mexico increases the risk of oil spills. A monitoring system is essential to improve the safety and reduce the risk of offshore oil and gas operations and systems. This project focused on developing an acoustic technique to detect, locate, and characterize oil spills in laboratory studies. During the project, it was found that (1) oil leakages can generate underwater sounds through bubble oscillations, which can be detected remotely by hydrophones, (2) the underwater sounds can be employed to provide useful information to assess the degree of oil leakages, and (3) the positions of the oil leakages can be determined through a hydrophone network using the developed localization techniques. In the future research, the gained scientific knowledge, detection metrics, oil-leakage characterization, and localization technology could be applied to develop a

prototype hydrophone network-based real-time monitoring system that would cover a large area of ocean at low cost.

Outcomes Achieved During the Project
This grant has provided a great opportunity to exploit the advantages of both underwater acoustic sensing and oil spill-induced underwater sound mechanisms, along with advanced localization techniques.

During the project, we achieved the following outcomes:
1) The underwater sounds generated by oil leakage are dominated by bubble oscillations rather than jet streaming. Also, the bubble sounds can be detected remotely by hydrophones.
2) The underwater sound information can be processed and analyzed to reveal causative properties of oil leakages such as crack size, flow rate, jet velocity, and bubble size distribution.
3) The developed localization techniques can determine the positions of bubble sources with satisfactory accuracy, even under multipath/reverberation and near-field conditions of the water tank.
4) For a more realistic investigation of oil spill events, a field test site with a large area is needed to perform oil leakage localization using conventional algorithms, such as the TDOA-based, DOA-based and energy-based methods, and other advanced algorithms, such as neutral networks and MFP methods.
5) With the scientific knowledge gained from this project, including detection metrics, oil-leakage characterization, and localization technology, a prototype, network-based hydrophone monitoring system could be developed for field use. With follow-on funding, investigators of this project team, in collaboration with industry stakeholders, could pursue development and deployment of an in-situ detection and localization system at Sardis Lake, which is just12 miles away from the University of Mississippi.

Communications, Outreach, and Dissemination Activities of Project
Three press releases about the project were published in the following two websites and one newspaper:
- https://www.usatoday.com/story/news/2017/12/27/ole-miss-researchers-using-acoustics-spot-underseaoilleaks/981894001
- https://news.olemiss.edu/um-researchers-receive-591000-grant-for-oil-leak-technology
- Oxford Citizen, Dec., 21, 2017, "UM researchers working on acoustic detection for undersea oil leaks".

We have built a website that summarizes the project including research background, research tasks, latest results, publications, references, and news and events: http://aduolp.olemiss.edu

We have presented project results in Gulf of Mexico Oil Spill & Ecosystem Science Conference, 178th Meeting of the Acoustical Society of America, and 22nd Annual Gulf of Mexico Deepwater Technical Symposium.

- Likun Zhang, Xudong Fan, Zhiqu Lu, "Characterization of sound induced by bubbles released from nozzles", Gulf of Mexico Oil Spill & Ecosystem Science Conference, Feb. 3-6, 2020, Tampa, FL

- Xing Yang, Lei Cao, Zhiqu Lu, "Characterization and localization of oil leakages using passive acoustic techniques", Gulf of Mexico Oil Spill & Ecosystem Science Conference, Feb. 3-6, 2020, Tampa, FL
- Likun Zhang, Xudong Fan, Zhiqu Lu, "Characterization of sound induced by bubbles released from nozzles", 178th ASA 2-7 Dec, 2019, San Diego, CA
- Zhiqu Lu, Raviteja Chinnambeti, and Lei Cao, "Localization of bubble sources in a water tank for oil spill detection", 22nd Annual Gulf of Mexico Deepwater Technical Symposium, Aug. 27-29, New Orleans, LA, 2018.

One manuscript was submitted to J. Acouti. Soc. AM-Ex. Lett and under review:
- Zhiqu Lu, Xudong Fan, and Likun Zhang, "A laboratory study of acoustic behaviors of bubbles caused by oil leakages", J. Acouti. Soc. AM-Ex. Lett. 2020 (under review).

One manuscript was prepared.
- Raviteja Chinnambeti, Lei Cao, and Zhiqu Lu, "Localization of a bubble source in water tank for oil spill detection".

Figures
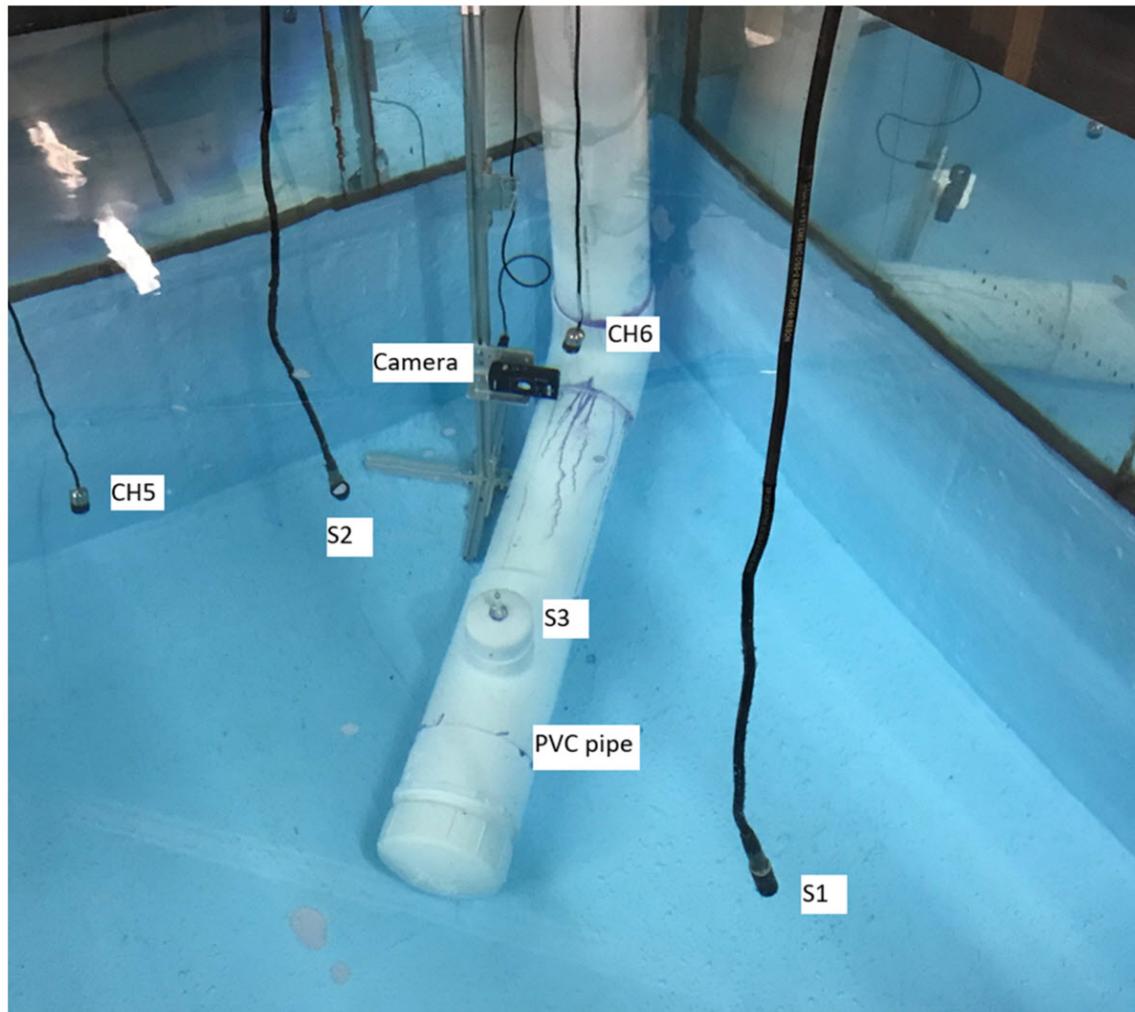
Figure 1-1: Photo of the water tank.
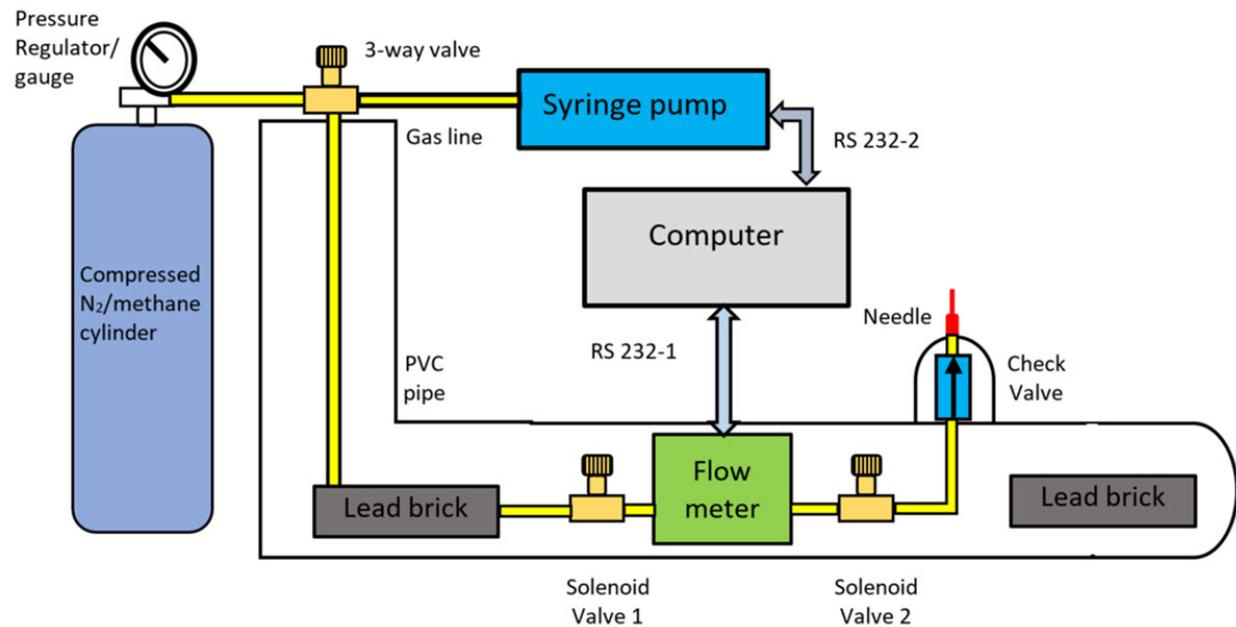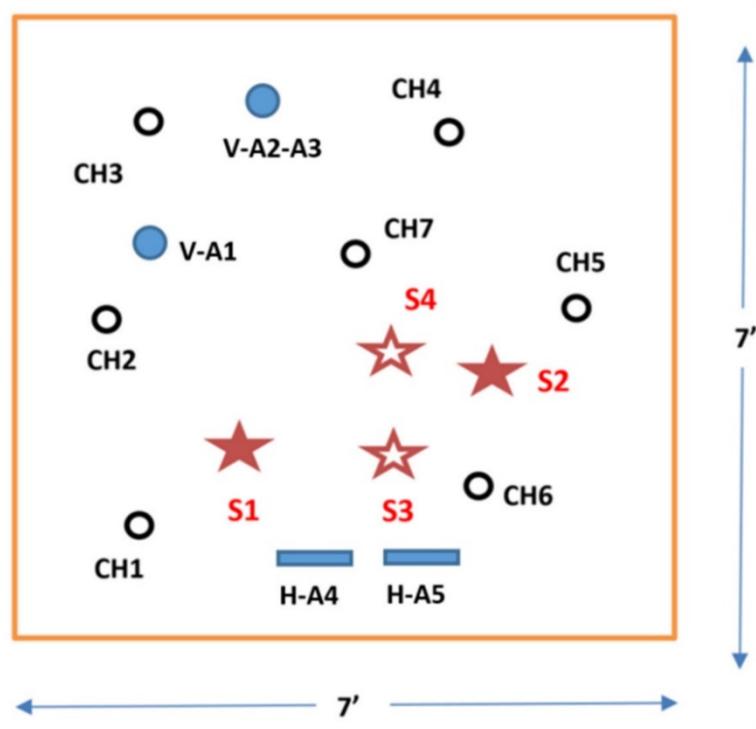
Figure 1-2: Experimental setup.

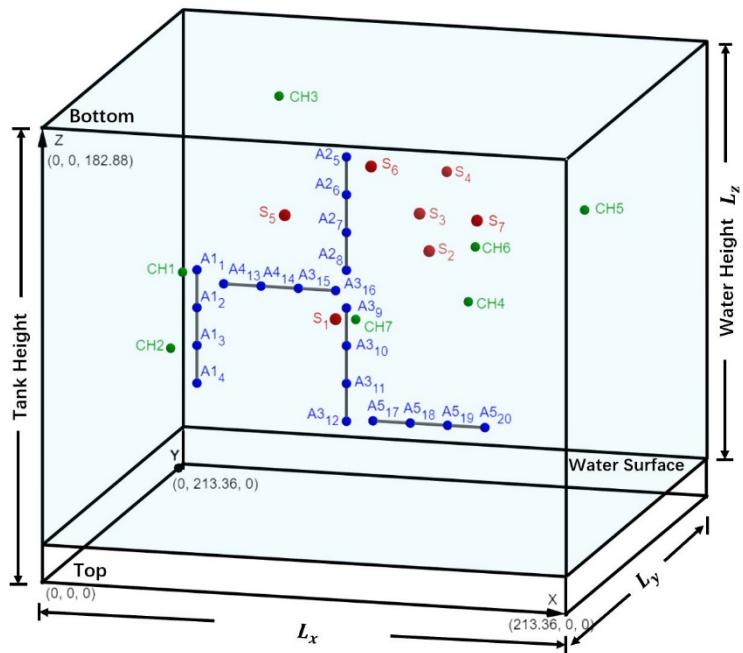**Figure 1-3a:** Top view of the hydrophone positions.

Figure 1-3b: Three-dimensional view of the hydrophone positions.

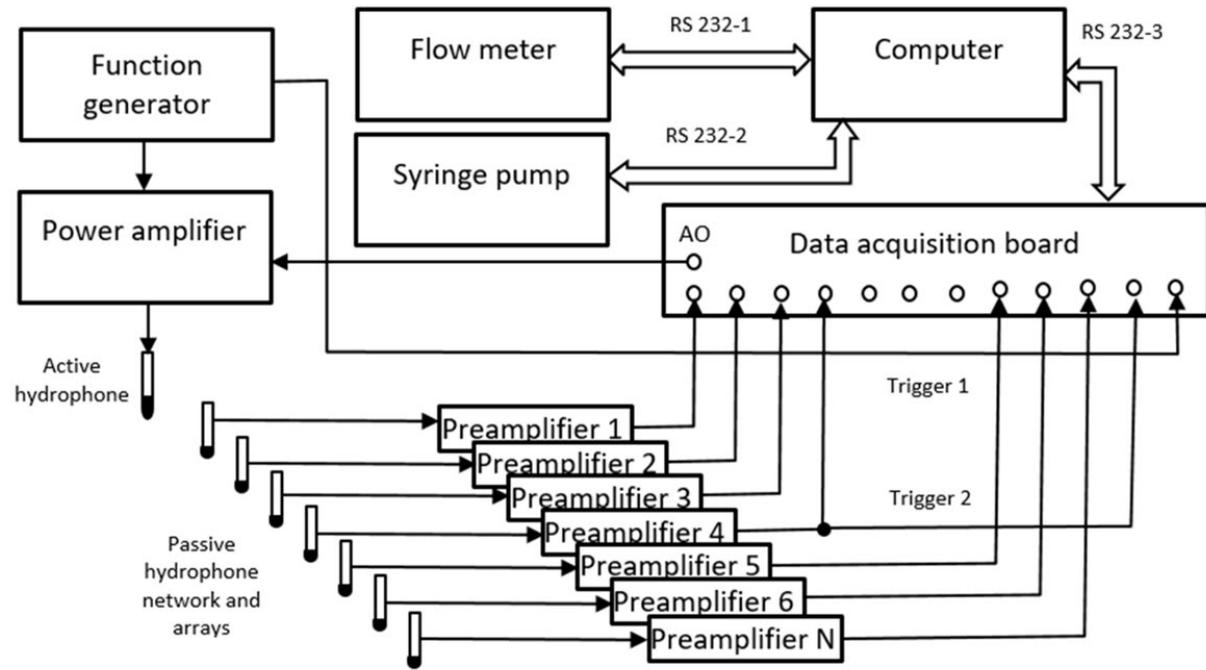**Figure 1-3**: **(a)** Top view and **(b)** three-dimensional view of the hydrophone positions.

Figure 1-4: Instrument control and data acquisition system.
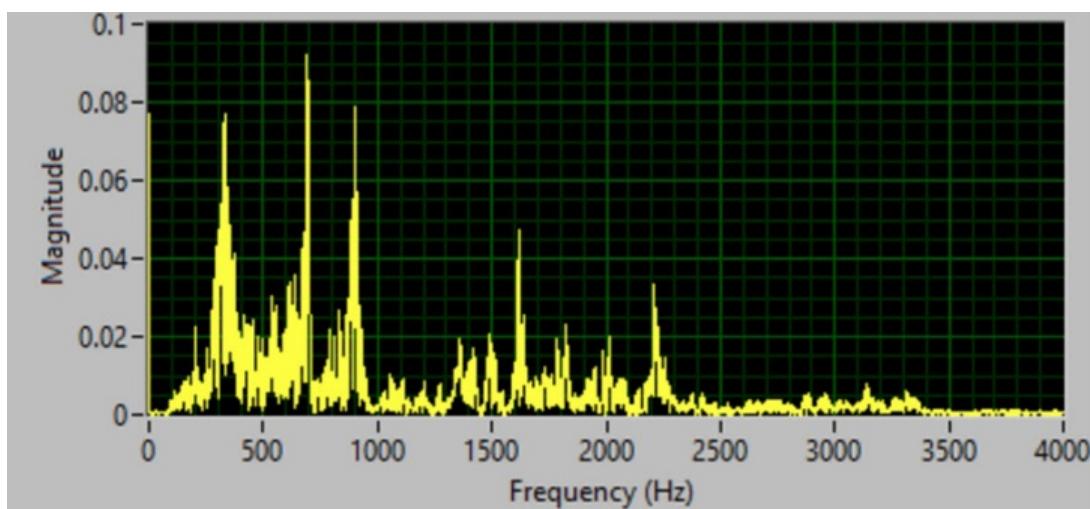
Figure 1-5a: constant flow bubbles photo.
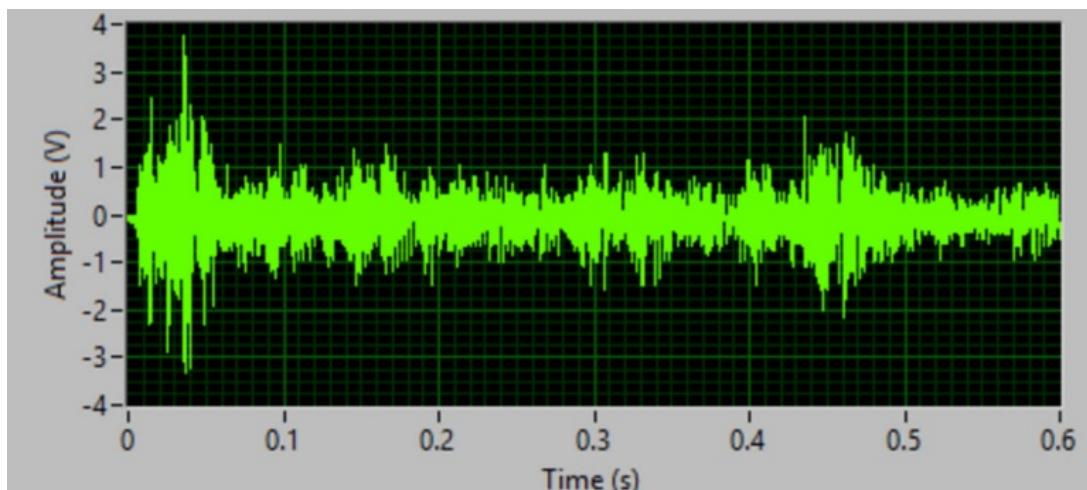

Figure 1-5b: constant flow sound.

Figure 1-5c: constant flow spectrum.

Figure 1-5: Constant flow bubbles **(a)** photo, **(b)** sound, and **(c)** spectrum.
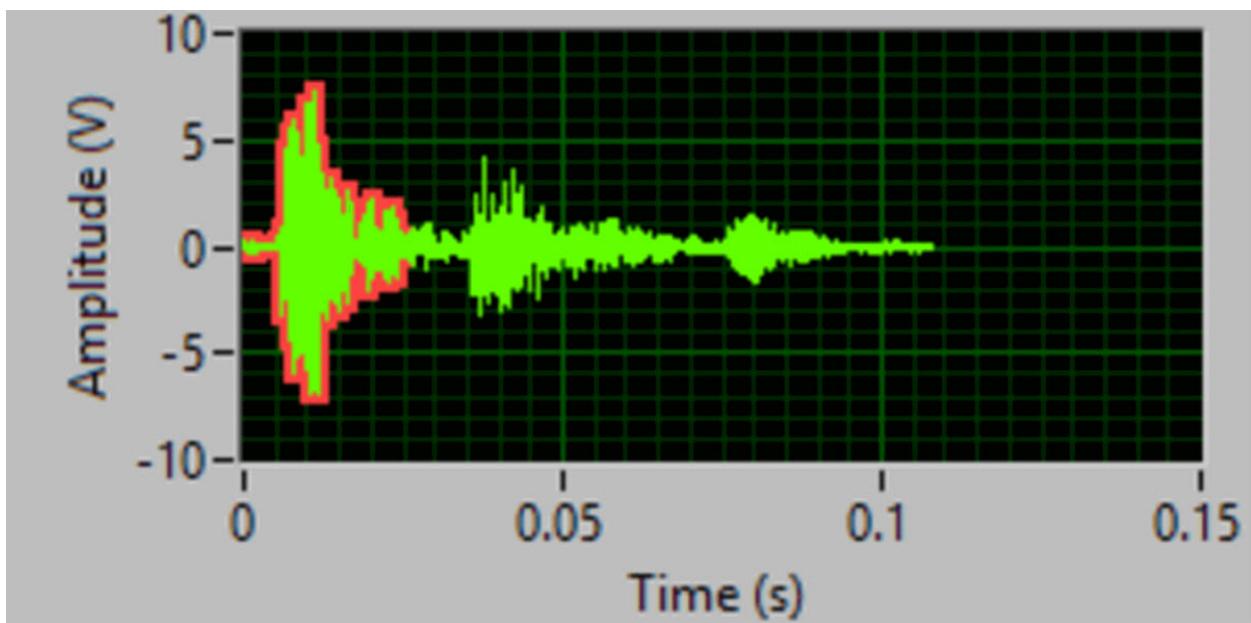
Figure 1-6a: A few bubbles photo.

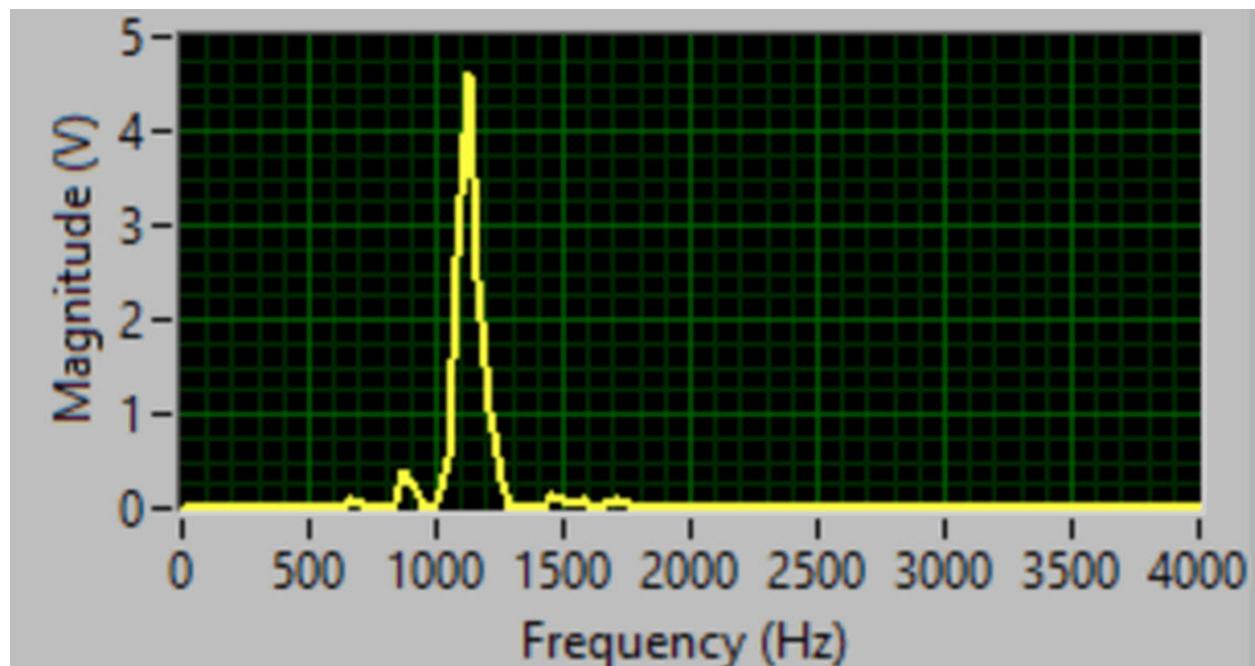**Figure 1-6b**: A few bubbles sound.

Figure 1-6c: A few bubbles spectrum.

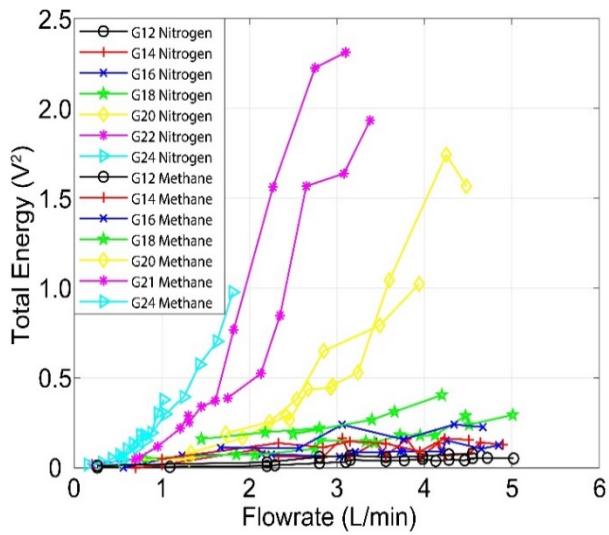**Figure 1-6**: A few bubbles (a) photo, (b) sound, and (c) spectrum.

Figure 2-1a: Total energy vs. flow rate.
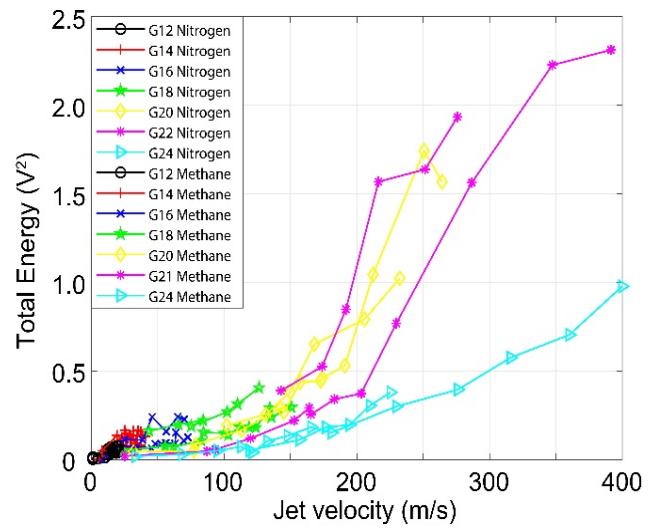
Figure 2-1b: Total energy vs jet velocity.
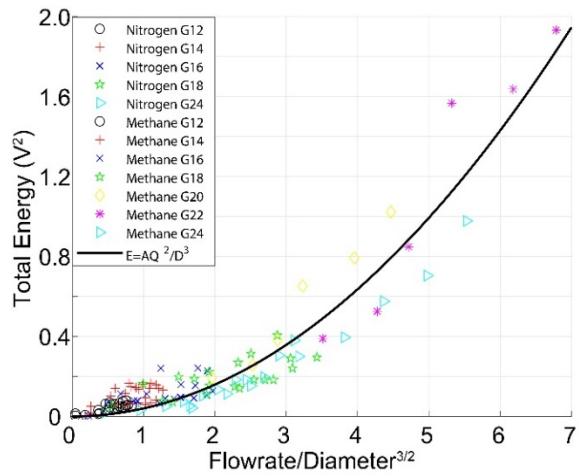
Figure 2-1c: Total energy as a function of flow flow rate and effective bubble radius.

Figure 2-1d: Total energy as a function of jet velocity and bubble generation rate.

Figure 2-1: Total energy (**a**) vs. flow rate, (**b**) vs. jet velocity, (**c**) as a function of flow rate and effective bubble radius, and (**d**) as a function of jet velocity and bubble generation rate.

Figure 2-2a: Resonant frequency histograms for nitrogen-1.
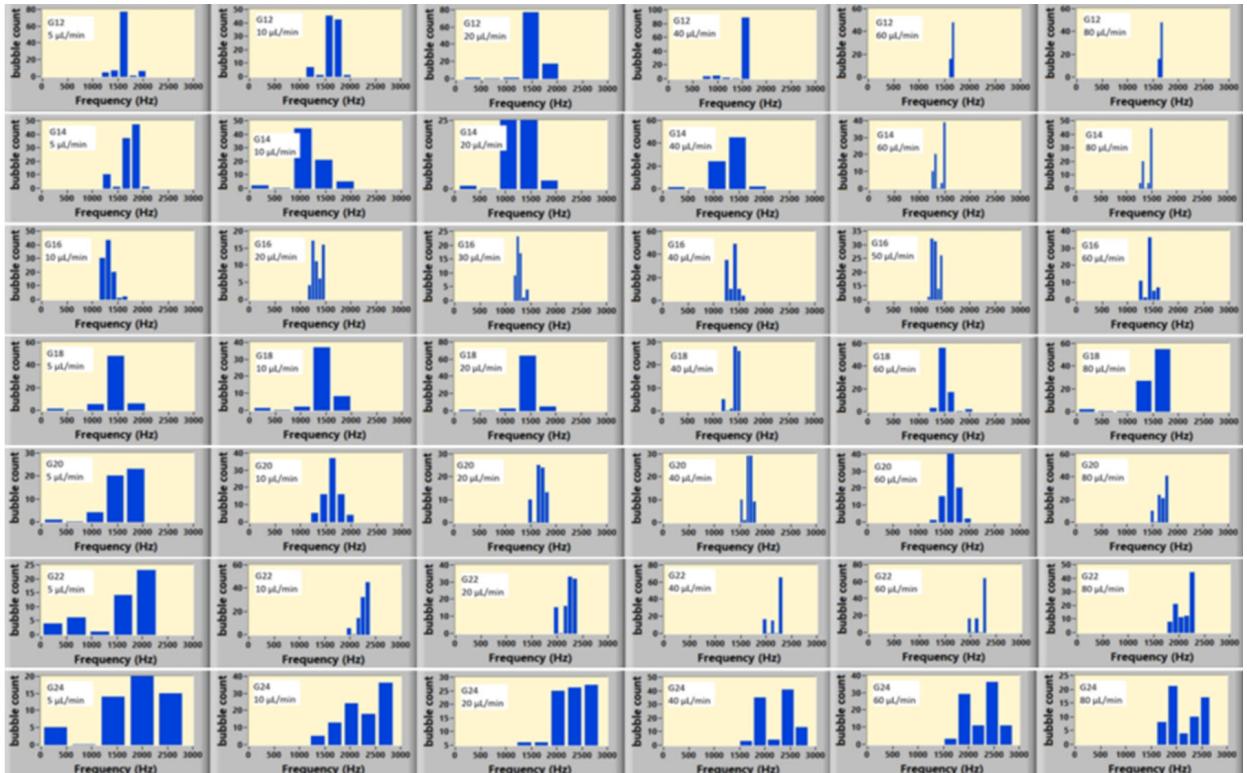
Figure 2-2b: Resonant frequency histograms for nitrogen-2.
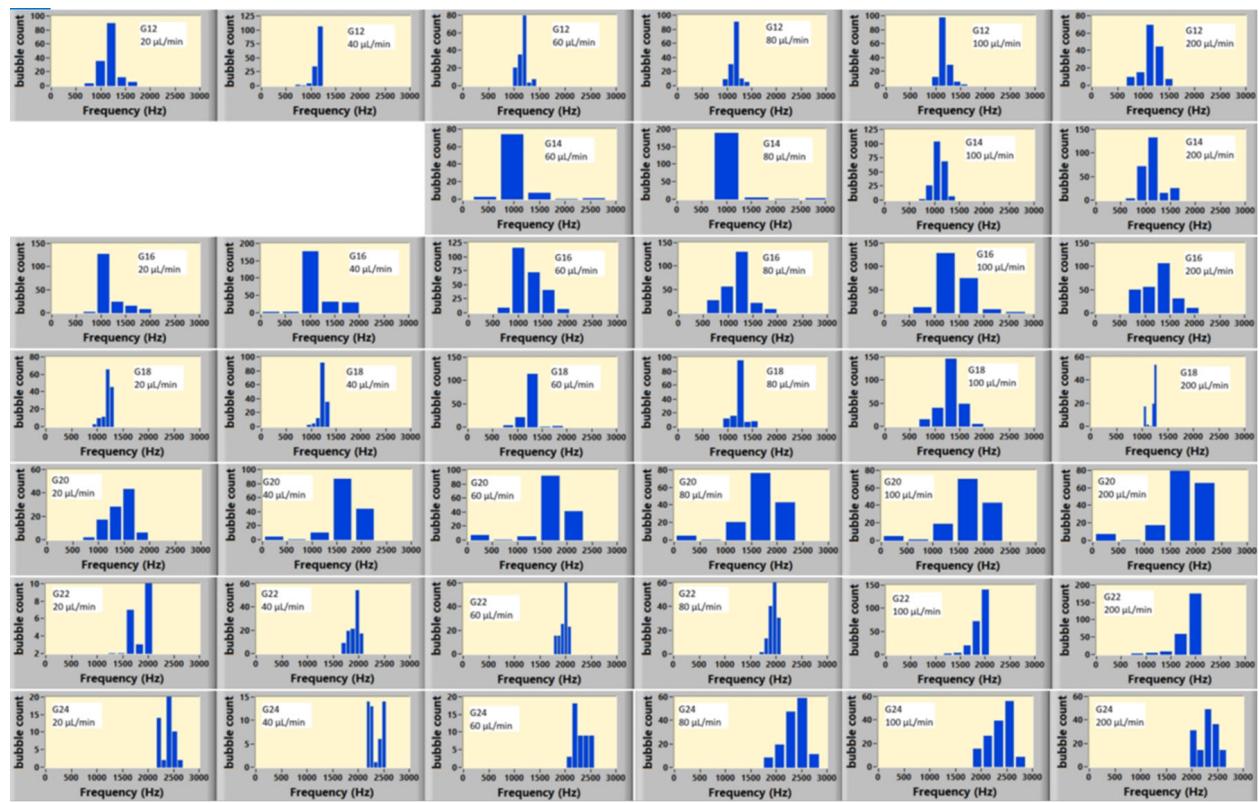
Figure 2-2c: Resonant frequency histograms for methane.

Figure 2-2: Resonant frequency histograms for (a) nitrogen-1, (b) nitrogen-2, and (c) methane.
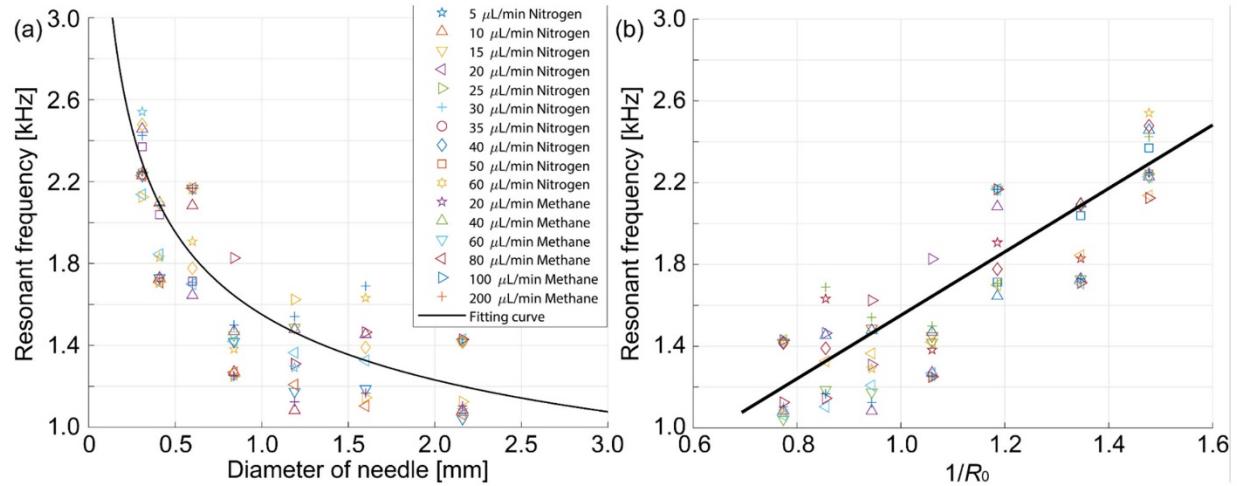
Figure 2-3a: Resonant frequency vs needle diameter.

Figure 2-3b: Resonant frequency vs inversed effective bubble radius.

Figure 2-3: resonant frequency vs (a) needle diameter and (b) inversed effective bubble radius.

Figure 2-4: Frequency spectrum vs bubble radius.

Figure 2-5: Bubble size distribution for nitrogen.
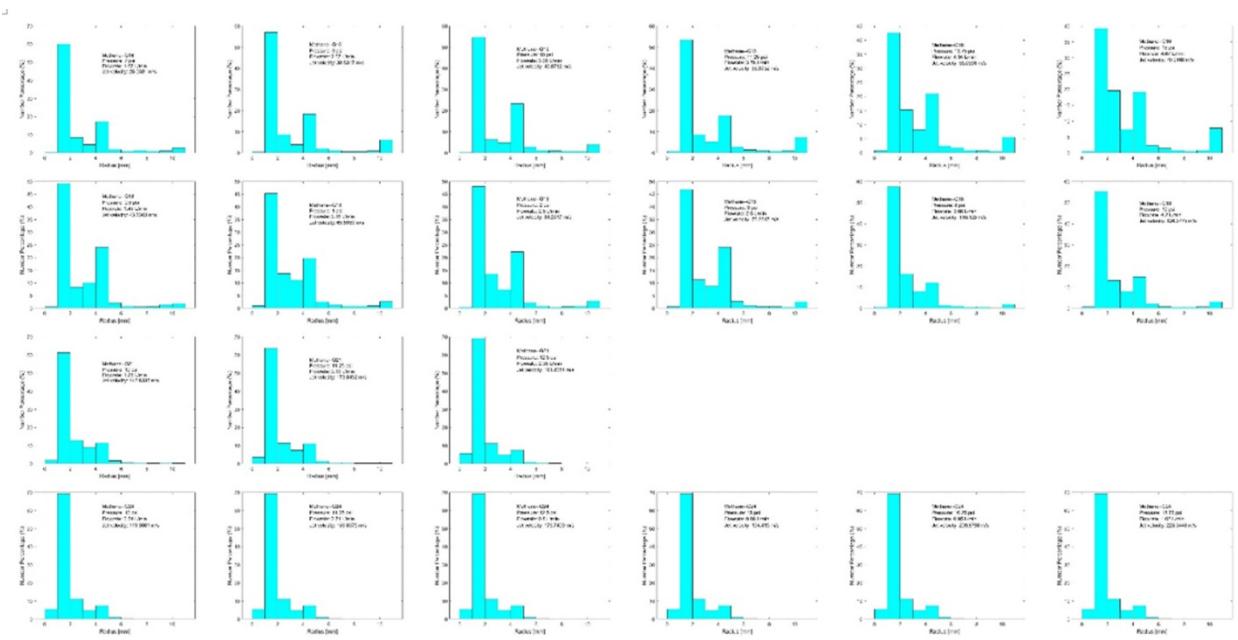
Figure 2-6: Bubble size distribution for methane.
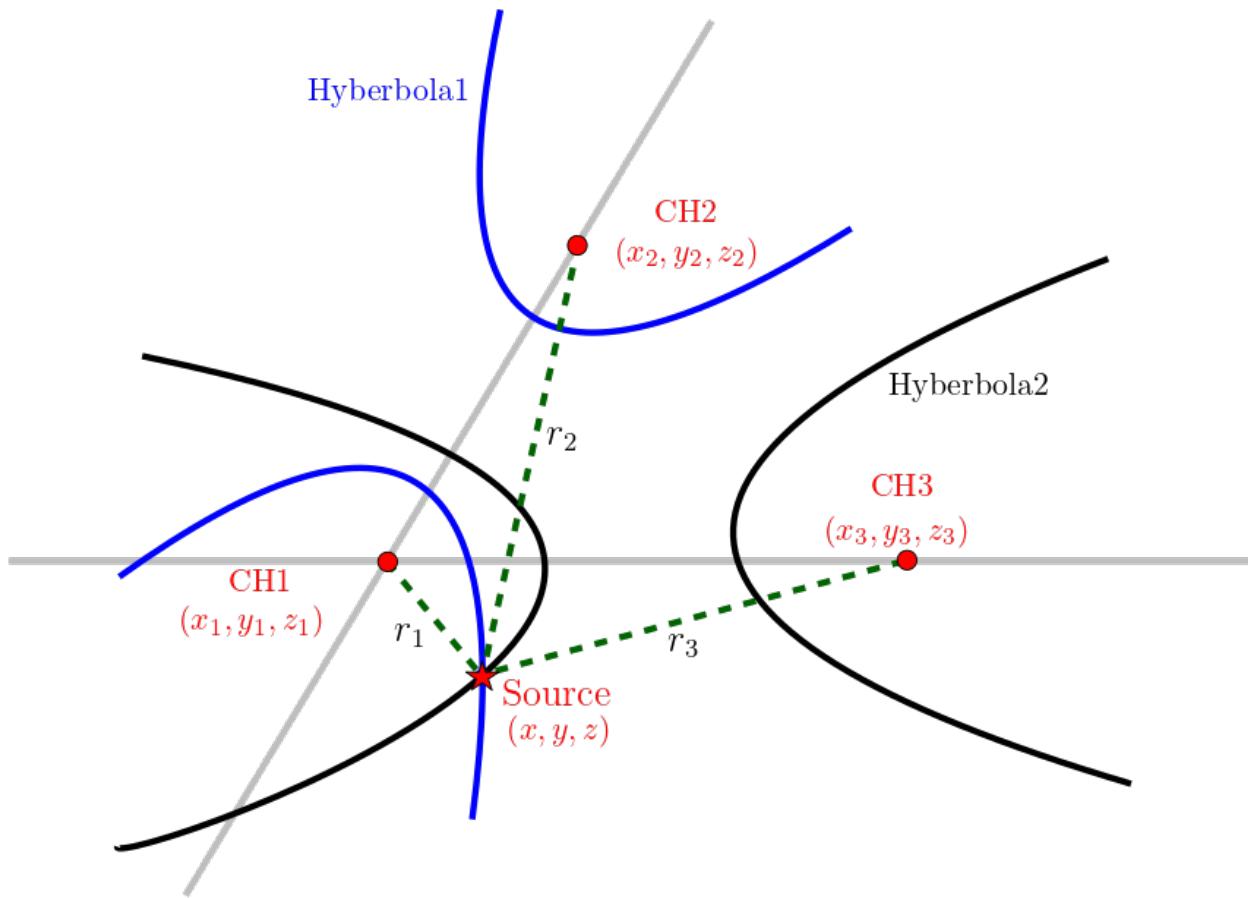
Figure 3-1: Time difference of arrival (TDOA) hyperbola.

```
        ┌─────────────┐
        │    Start    │
        └─────────────┘
               │
               ▼
┌─────────────────────────────────────────────┐
│  Sort 3-dimensional co-ordinates of anchor   │
│  nodes in ascending order of distance from   │
│              source node                     │
└─────────────────────────────────────────────┘
               │
               ▼
┌─────────────────────────────────────────────┐
│  Shift system coordinate so that the anchor  │
│  node closest to source (reference node)     │
│  becomes origin point (0,0,0)                │
└─────────────────────────────────────────────┘
               │
               ▼
┌─────────────────────────────────────────────┐
│  Obtain time difference of arrival between   │
│       anchor nodes and reference node        │
└─────────────────────────────────────────────┘
               │
               ▼
┌─────────────────────────────────────────────┐
│     Initialize the velocity of the sound     │
└─────────────────────────────────────────────┘
               │
               ▼
┌─────────────────────────────────────────────┐
│  Solve the linear least squares equations to │
│        get the source node location          │
└─────────────────────────────────────────────┘
               │
               ▼
┌─────────────────────────────────────────────┐
│       Shift system coordinate back           │
└─────────────────────────────────────────────┘
               │
               ▼
        ┌─────────────┐
        │    Stop     │
        └─────────────┘
```
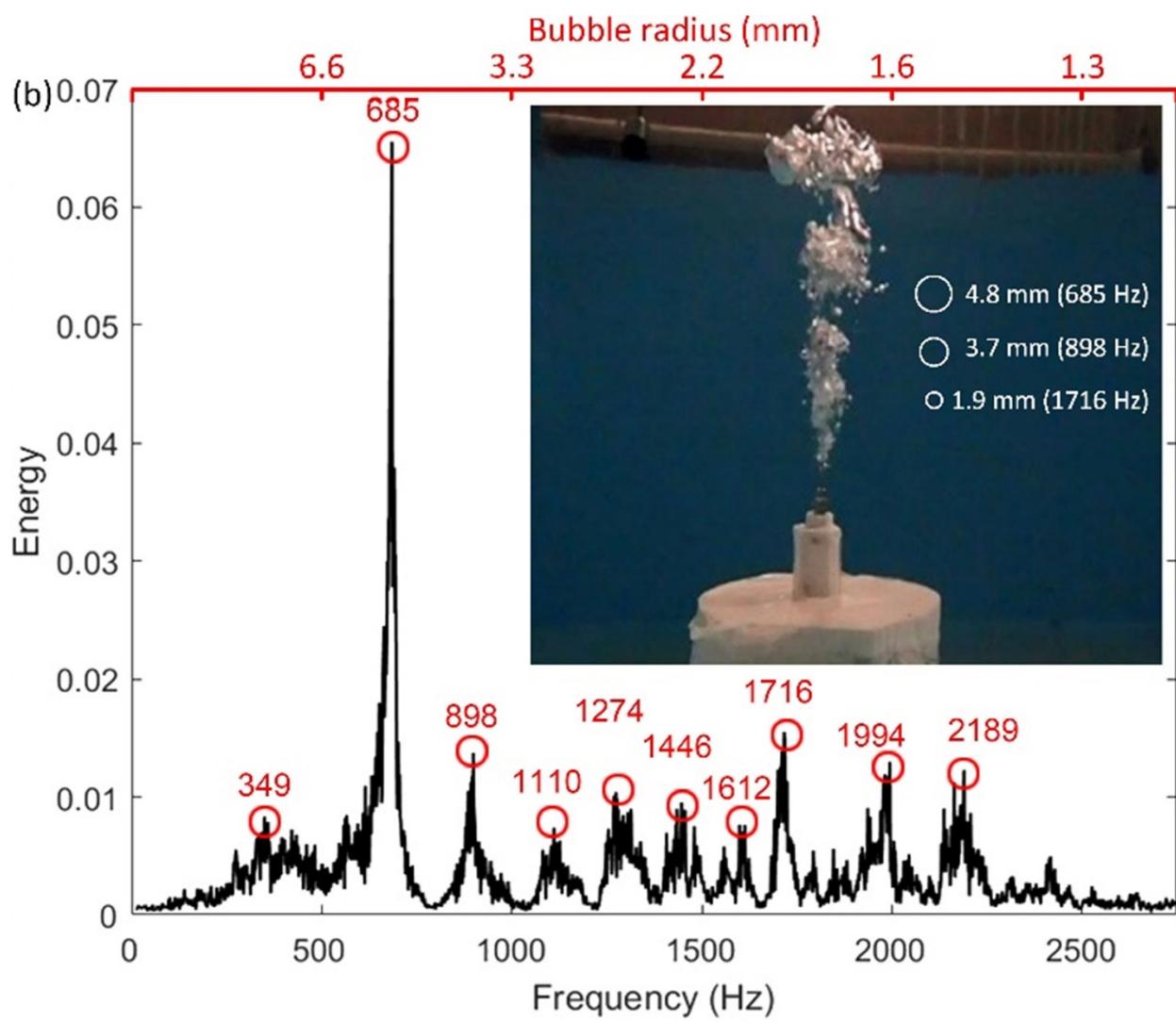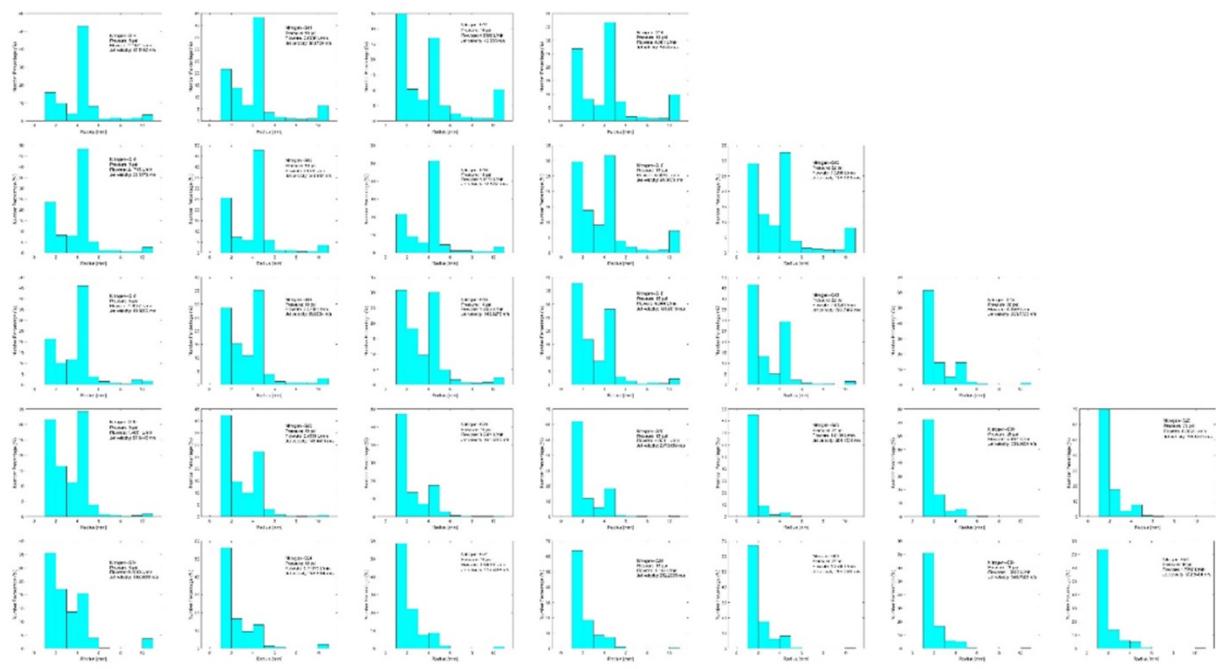
Figure 3-2: Flow chart for linear least square estimation.

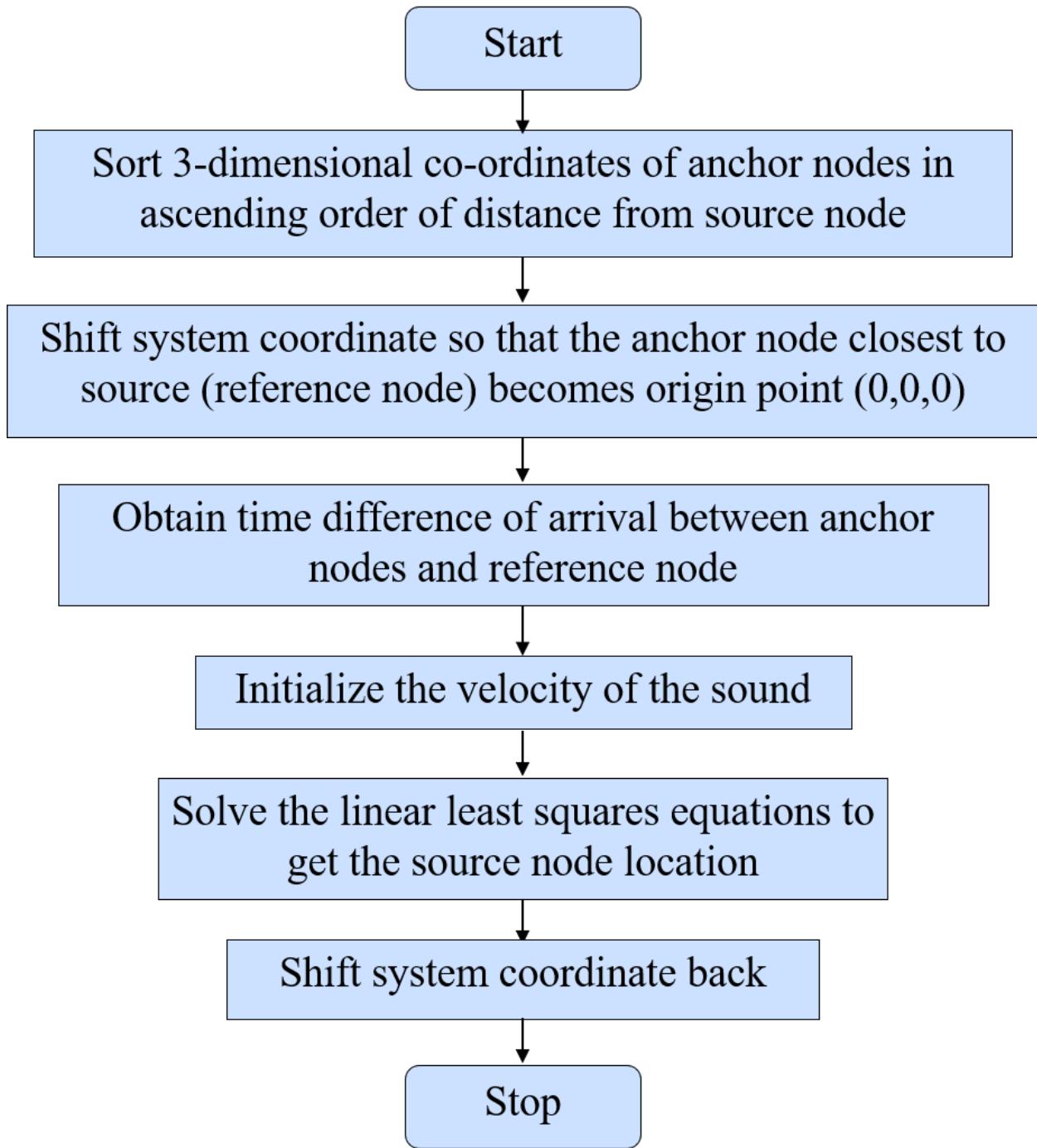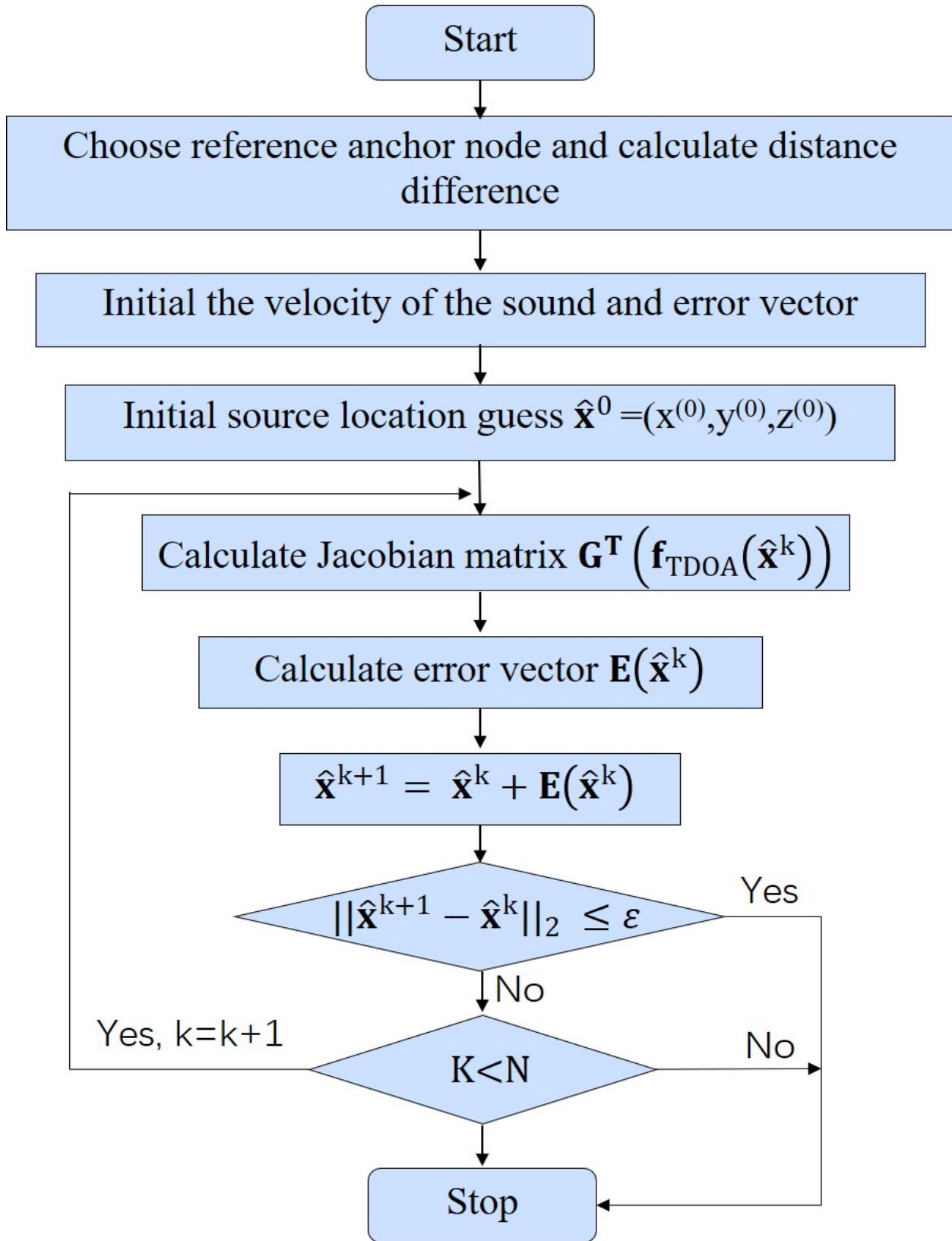**Figure 3-3**: Flow chart for nonlinear least square estimation.

Sources	Signal Type	True Location (cm)	Estimated Location (cm)		RMSE (cm)	
			LLSE	NLS	LLSE	NLS
S1	Electric	(89.8, 66.3, 121.0)	(88.70, 68.92, 112.40)	(89.62, 70.70,111.96)	5.24	5.82
S2	Electric	(177.0, 74.5, 141.5)	(175.53, 78.05, 138.10)	(174.90, 79.01,137.59)	2.96	3.65
S3	Bubble	(139.8, 52.5, 145.5)	(137.87, 52.70, 139.66)	(138.49, 50.93,142.34)	3.54	2.16
S4	Bubble	(136.0,112.5,140.0)	(133.40,115.50,146.20)	(136.30,115.60,145.60)	4.25	3.70

Figure 3-4: Source position estimations using time difference of arrival method.

Figure 3-5: Swimming pool test.

Algorithm Framework of spectra ratio-based localization

Input:

1: The water tank and grids dimension, receivers' location and number

2: The recorded signal by receivers, $p_i, i = 1, \dots, 7$

Output:

3: Calculate three different model's* Green's functions dictionary with help of step1, $G(\vec{r}_i, \vec{r}_s, \omega)$

4: Transfer p_i to frequency domain $P_i(\omega)$ with interested frequency range 600Hz to 2KHz.

5: Calculate spectra ratio $S_{m,n}(\vec{r}_s, \omega)$ with help of $G(\vec{r}_i, \vec{r}_s, \omega)$ and $P_i(\omega)$

6: calculate the rms of $S_{m,n}(\vec{r}_s, \omega)$ in dB scale

7: Calculate detection factor of all receivers with help of step 6

8: Estimation result is $\vec{r}_s$ which maximize detection factor

9: **return** $\vec{r}_s$

* M1 means traditional 'Dirichlet Model', M2 means 'Including Leakage Through the Walls Model', proposed means 'Proposed New Water Tank model'.

Figure 3-6: Framework of spectra ratio (Green function)-based localization algorithm.

Bubble Source S7	Model	X [m]	Y [m]	Z [m]	RMSE [m]
True Location		1.465	1.135	1.290	
Estimated Location	Proposed	1.600	1.173	1.091	0.141

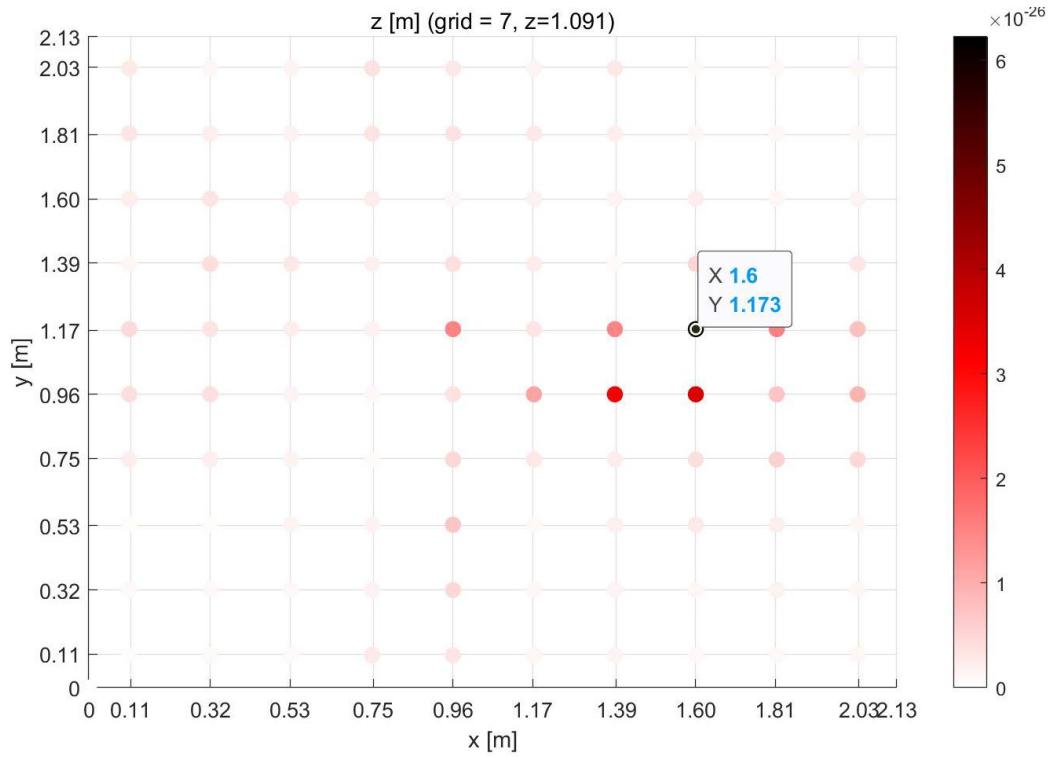**Figure 3-7**: Source position estimation using spectra-ratio method.

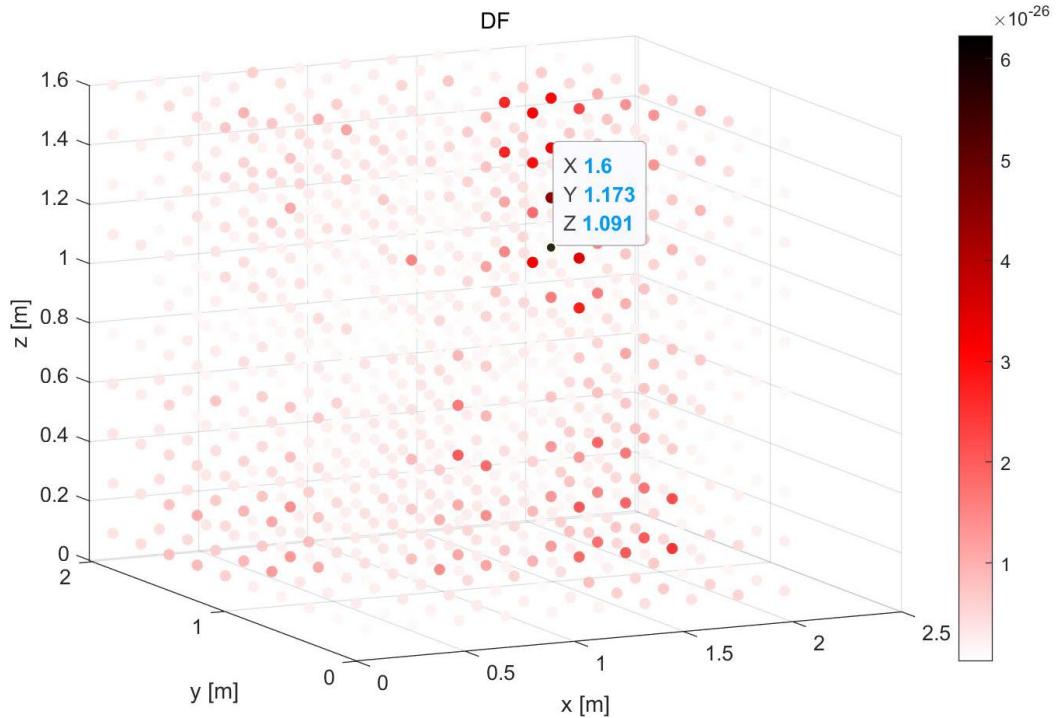**Figure 3-8a:** Two-dimensional displays of the detection factor.

Figure 3-8b: Three-dimensional displays of the detection factor.

Figure 3-8: (a) Two-dimensional and (b) three-dimensional displays of the detection factor.

Bubble Sources		Model	X [m]	Y [m]	Z [m]	RMSE [m]
S4	True Location		1.460	1.120	1.480	
	Estimated Location	M1	1.600	0.960	1.427	0.127
		M2	1.387	0.960	1.427	0.106
		Proposed	1.387	0.960	1.595	0.121
S5	True Location		0.710	1.030	1.290	
	Estimated Location	M1	0.533	1.173	1.595	0.220
		M2	0.533	1.173	1.595	0.220
		Proposed	0.533	1.173	1.595	0.220
S6	True Location		1.020	1.185	1.470	
	Estimated Location	M1	0.960	0.960	0.084	0.811
		M2	0.960	1.173	0.420	0.607
		Proposed	0.960	1.173	1.091	0.222
S7	True Location		1.465	1.135	1.290	
	Estimated Location	M1	1.600	0.960	1.427	0.150
		M2	1.387	0.960	1.091	0.159
		Proposed	1.600	1.173	1.091	0.141

Figure 3-9: Several source position estimations using spectra-ratio method with three water tank models.

Bibliography

Leighton, T. G., & Walton, A. J. (1987). An experimental study of the sound emitted from gas bubbles in a liquid. *European Journal of Physics*, *8*(2), 98–104. https://doi.org/10.1088/0143-0807/8/2/005

Longuet-Higgins, M., Kerman, B. R., & Lunde, K. (1991). The release of air bubbles from an underwater nozzle. *The Journal of the Acoustical Society of America*, *89*(4B), 2014. https://doi.org/10.1121/1.2029902

Minnaert, M. (1933). On musical air-bubbles and the sounds of running water. *The London, Edinburgh, and Dublin Philosophical Magazine and Journal of Science*, *16*(104), 235–248. https://doi.org/10.1080/14786443309462277

Novak, A., Bruneau, M., & Lotton, P. (2018). Small-Sized Rectangular Liquid-Filled Acoustical Tank Excitation: A Modal Approach Including Leakage Through the Walls. *Acta Acustica United with Acustica*, *104*(4), 586–596. https://doi.org/10.3813/aaa.919199

Novak, A., Cisar, P., Bruneau, M., Lotton, P., & Simon, L. (2019). Localization of sound-producing fish in a water-filled tank. *The Journal of the Acoustical Society of America*, *146*(6), 4842–4850. https://doi.org/10.1121/1.5138607

Data Report

DataType	DigitalResourceType	Title	FileName	Creators	PointofContact	PublicationYear	RepositoryName	DOIorPersistentURL	Keywords	Publications
Engineering	*Tabular/Spreadsheet*	active hydrophone tests	Tank-18-10-02-09-53-44-S1-500 kHz.xls	Lu, Zhiqu	zhiqulu@olemiss.edu 662-915-5660	2018	UM BOX and UM eGROVE	https://egrove.olemiss.edu/	Active hydrophone, underwater signals	N/A
Engineering	Tabular/Spreadsheet	nitrogen-constant flow tests	Tank-18-10-08-10-52-38-G14-cons-2.5psi-100 kHz - Gain100.xls	Lu, Zhiqu	zhiqulu@olemiss.edu 662-915-5660	2018	UM BOX and UM eGROVE	https://egrove.olemiss.edu/	nitrogen, underwater signals	N/A
Engineering	Tabular/Spreadsheet	nitrogen-a few bubble tests	Tank-18-07-30-08-12-50-G18-single-30uL-250 kHz.xls	Lu, Zhiqu	zhiqulu@olemiss.edu 662-915-5660	2018	UM BOX and UM eGROVE	https://egrove.olemiss.edu/	nitrogen, underwater signals	N/A
Engineering	Video	nitrogen-constant flow video	G16-5 PSI.mov	Lu, Zhiqu	zhiqulu@olemiss.edu 662-915-5660	2018	UM BOX and UM eGROVE	https://egrove.olemiss.edu/	nitrogen, constant flow video	N/A
Engineering	Video	nitrogen-a few bubble video	G16-single bubble-1.mov	Lu, Zhiqu	zhiqulu@olemiss.edu 662-915-5660	2018	UM BOX and UM eGROVE	https://egrove.olemiss.edu/	nitrogen, a few bubble video	N/A
Engineering	Images	nitrogen-histograms	Tank-18-08-09-09-12-24-G16-single-60uL-250 kHz.jpg	Lu, Zhiqu	zhiqulu@olemiss.edu 662-915-5660	2018	UM BOX and UM eGROVE	https://egrove.olemiss.edu/	nitrogen, resonat frequency, histograms	N/A
Engineering	Tabular/Spreadsheet	nitrogen-total energy vs flow rate	Total energy vs pressure.xls	Lu, Zhiqu	zhiqulu@olemiss.edu 662-915-5660	2018	UM BOX and UM eGROVE	https://egrove.olemiss.edu/	nitrogen, total energy, flow rate	N/A
Engineering	Tabular/Spreadsheet	nitogen-total energy vs jet velocity	Total energy vs pressure.xls	Lu, Zhiqu	zhiqulu@olemiss.edu 662-915-5660	2018	UM BOX and UM eGROVE	https://egrove.olemiss.edu/	nitogen, total energy, jet velocity	N/A
Engineering	Tabular/Spreadsheet	Localization	The results of localization.xls	Cao, Leo	lcao@olemiss.edu 662-915-5389	2018	UM BOX and UM eGROVE	https://egrove.olemiss.edu/	Localization	N/A
Engineering	Tabular/Spreadsheet	Modeling	Sound frequency and bubble size for different needles.xls	Zhang, Likun	zhang@olemiss.edu 662-915-7046	2018	UM BOX and UM eGROVE	https://egrove.olemiss.edu/	Resonant frequency, needle size	N/A
Engineering	Tabular/Spreadsheet	nitrogen-total energy vs flow rate	total energy and flow rate-2.xlsx	Lu, Zhiqu	zhiqulu@olemiss.edu 662-915-5660	2019	UM BOX and UM eGROVE	https://egrove.olemiss.edu/	nitrogen, total energy, flow rate	N/A
Engineering	Tabular/Spreadsheet	nitogen-total energy vs jet velocity	total energy and flow rate-2.xlsx	Lu, Zhiqu	zhiqulu@olemiss.edu 662-915-5660	2019	UM BOX and UM eGROVE	https://egrove.olemiss.edu/	nitogen, total energy, jet velocity	N/A
Engineering	Tabular/Spreadsheet	methane-constant flow tests	Tank-18-11-12-09-33-24-G18-CH4-5psi-100 kHz - Gain100 - 40dB.xls	Lu, Zhiqu	zhiqulu@olemiss.edu 662-915-5660	2019	UM BOX and UM eGROVE	https://egrove.olemiss.edu/	methane, underwater signals	N/A
Engineering	Tabular/Spreadsheet	methane-a few bubble tests	Tank-18-11-28-22-33-55-200ul-G16-single-250 kHz-Gain1000-60dB.xls	Lu, Zhiqu	zhiqulu@olemiss.edu 662-915-5660	2019	UM BOX and UM eGROVE	https://egrove.olemiss.edu/	methane, underwater signals	N/A
Engineering	Images	methane-resonant frequency histograms	Tank-18-11-28-22-39-09-100ul-G16-single-250 kHz-Gain1000-60dB.jpg	Lu, Zhiqu	zhiqulu@olemiss.edu 662-915-5660	2019	UM BOX and UM eGROVE	https://egrove.olemiss.edu/	methane, resonant frequency, histograms	N/A
Engineering	Tabular/Spreadsheet	methane-total energy vs flow rate	total energy and flow rate-methane.xlsx	Lu, Zhiqu	zhiqulu@olemiss.edu 662-915-5660	2019	UM BOX and UM eGROVE	https://egrove.olemiss.edu/	methane, total energy, flow rate	N/A
Engineering	Tabular/Spreadsheet	methane-total energy vs jet velocity	total energy and flow rate-methane.xlsx	Lu, Zhiqu	zhiqulu@olemiss.edu 662-915-5660	2019	UM BOX and UM eGROVE	https://egrove.olemiss.edu/	methane, total energy , jet velocity	N/A
Engineering	Text	total energy vs effective bubble number	Energy_total.m	Zhang, Likun	zhang@olemiss.edu 662-915-7046	2020	UM BOX and UM eGROVE	https://egrove.olemiss.edu/	total energy, effective bubble number	N/A
Engineering	Text	resonant frequency vs needle diameter	Theory_single_bubble.m	Zhang, Likun	zhang@olemiss.edu 662-915-7046	2021	UM BOX and UM eGROVE	https://egrove.olemiss.edu/	resonant frequency, needle diameter	N/A

InfoProductType	DigitalResourceType	Title	FileName	Creators	PublicationYear	Publisher	RepositoryName	DOIorPersistentURL	DatasetReference
Website or Data Portals	Web Based Resource	Acoustic detection for undersea oil leak project	N/A	Lu, Zhiqu	2018	NCPA, UM	N/A	N/A	http://aduolp.olemiss.edu/